Electrochemical Detection of Anti-Biofilm Activity Using Unnatural Amino Acid-Containing Antimicrobial Peptides

By Sergey M. Vinogradov

May 2015

Director of Thesis: Eli G. Hvastkovs

Major Department: Chemistry

Bacterial infections are a significant health problem that can be detrimental to the human population. It is estimated that bacterial infections are responsible for billions of dollars' worth of damages in the health care field alone, and numerous deaths annually. Bacterial infections can become so detrimental because they produce a structure called biofilm, which facilitates antibiotic resistance and is a major cause of chronic infections. In order to combat this threat, new anti-biofilm and antibiotic therapies are being developed and their efficiency must be tested. A series of antimicrobial peptides (AMP) containing unnatural Tic-Oic amino acids have been developed for this purpose.

Traditional methods such as biological assays are the standard by which antibiotics are judged, but they have their drawbacks, such as the lengthy test times and the costs associated with it and the reagents. Electrochemical biosensors can remedy some of those drawbacks by offering speed and cost benefits. Electrochemical biosensors consisting of Layer-by-Layer (LbL) modified electrodes were constructed. These sensors were fabricated to test the anti-biofilm activity of the aforementioned unnatural amino acid-containing antimicrobial peptides

against a model of *Pseudomonas aeruginosa* or against the bacteria itself. *P. aeruginosa* is a common biofilm producing bacteria.

First, we employed alginate as one of the layers in our sensor as *P. aeruginosa* is known to produce this as its major biofilm component. We show that the penetration of the alginate layer by the AMP can be detected electrochemically utilizing a solution-phase redox active molecule that produces an increasing signal upon electrochemical reduction when the film becomes compromised. Biological assays are presented that provide some validation for the sensor, but elucidated a particular AMP as compared to the electrochemical alginate sensor.

Based on this slight disagreement between our electrochemical model and the biological assay, we employed sensors that featured directly immobilized *P. aeruginosa* PAO1 on the electrode surface. These bacteria are electroactive, which negated the need for an external redox active molecule, and allowed the monitoring of anti-biofilm activity via a signal decrease over time. The *P. aeruginosa* sensor showed more agreement with the biological assay, highlighting the same AMP as active toward biofilm degredation at low (<1 μM) concentrations. Overall, these electrochemical biosensors utilizing models of and actual *P. aeruginosa* have opened up new avenues to test for effectiveness of potential anti-biofilm agents toward biofilm forming bacteria.

Electrochemical Detection of Anti-Biofilm Activity Using Unnatural Amino Acid-Containing Antimicrobial Peptides

A Thesis

Presented To the Faculty of the Department of Chemistry

East Carolina University

In Partial Fulfillment of the Requirements for the Degree

Masters of Science in Chemistry

By

Sergey M. Vinogradov

May 2015

Electrochemical Detection of Anti-Biofilm Activity Using Unnatural Amino Acid-Containing Antimicrobial Peptides

by

Sergey M. Vinogradov

APPROVED BY:

DIRECTOR OF THESIS: _____
Eli G. Hvastkovs, Ph.D.

COMMITTEE MEMBER: _____
Allison S. Danell, Ph.D.

COMMITTEE MEMBER: _____
Eric Anderson, Ph.D.

COMMITTEE MEMBER: _____
Colin S. Burns, Ph.D.

CHAIR OF THE DEPARTMENT OF CHEMISTRY: _____
Allison S. Danell, Ph.D.

DEAN OF THE GRADUATE SCHOOL: _____
Paul Gemperline, Ph.D.

ACKNOWLEDGEMENTS

I would never have been able to finish my thesis without the guidance of my committee members, and support from my family, wife and daughter.

I would like to express my deepest gratitude to my advisor, Dr. Eli Hvastkovs, for his guidance, patience, and providing me with the skills to complete this project. I would like to thank Dr. Anderson, who supported my research and taught me the biological aspects of this project. I would also like to thank my thesis committee members Dr. Danell and Dr. Burns.

Finally, I would like to thank my wife and daughter, Amanda and Zoe Vinogradov. They were always there supporting me. I would also like to thank my parents, sisters and grandparents who have never let me give up.

TABLE OF CONTENTS

LIST OF TABLES

LIST OF SCHEMES

LIST OF FIGURES

LIST OF SYMBOLS AND ABBREVIATIONS

MRSA	Methicillin-resistant *Staphylococcus Aureus*
CF	Cystic Fibrosis
MDR	Multi-drug resistant
EPS	Exopolysaccharide
QS	Quorum sensing
AI	Autoinducer
AHLs	Acyl Homoserine Lactones
AMP	Antimicrobial peptides
Tic	Tetrahydroisoquinolinecarboxylic acid
Oic	Octahydroindolecarboxyl acid
TTO	Tic Oic dipeptide unit containing peptide
ESKAPE	Known to commonly infect chronic wounds. These include *Eneterococcus faecium* (meningitis), *Straphyloccocus aureus* (boils, sinusitis), *Klebsiella pnemoniae (*pneumonia), *Acinetobacter baumanni* ("Iraqibacter"), *Pseudomonas aeruginosa* (opportunistic), and *Entrobacter* (opportunistic)
MIC	Minimum Inhibitory Concentration
MBC	Minimum Bacterial Concentration
SWV	Square wave voltammetry
CV	Cyclic voltammetry
HDME	Hanging mercury drop electrode
DPV	Differential pulse voltammetry

LBL	Layer-by-layer
E-buffer	10 mM Tris/10 mM NaCl pH 7.4, Electrochemical buffer
Tris	Tris(hydroxymethyl)amino methane buffer
PDDA	Poly(diallyldimethylammonium) chloride
PSS	Polystyrene sulfonate
LB	Luria broth
SCE	Saturated calomel electrode
Pirate media	Biofilm growth media
A	Ampere
°C	Celsius
L	Liter
Q	Charge (μC, C)
C	Coulomb
DI H_2O	Deionized water
DNA	Deoxyribonucleic acid
RNA	Ribonucleic acid
Ml	Microliter
μm	Micrometer
μM	Micromolar
mg	Milligram
ml	Milliliters
mm	Millimeters
mM	Millimolar

min	Minutes
M	Molar
mol	Moles
nm	Nanometer
nM	Nanomolar
Ar	Argon
I_p	Peak current ratio
Pt	Platinum wire
PAH	polycyclic aromatic hydrocarbon
E	Potential (V)
s	Seconds
Ag/AgCl	Silver/Silver chloride
NaCl	Sodium chloride
UV-Vis	Ultraviolet-Visible
V	Volts

CHAPTER 1: INTRODUCTION

Bacterial Biofilm and Traditional Treatment Regimens

Bacterial infections are a significant health problem that can be detrimental to the human population. It is estimated that bacterial infections are responsible for billions of dollars worth of damages and numerous human deaths annually.[1] However, the manner in which bacteria cause their problems can be much more nuanced. Bacteria can infect a host as free living cells, or planktonically, but as they grow they can aggregate and form secondary structures that make them much more problematic.[2,3] As bacteria come together and aggregate, they can form structures termed biofilms.[2-7] Some key biofilm forming bacteria that affect human health are summarized in Table 1.1. These bacteria include methicillin-resistant *Staphylococcus Aureus* (MRSA), and *Pseudomonas aeruginosa*, which is associated with chronic respiratory illness in cystic fibrosis (CF) patients. The NIH estimates that 3 out of 4 bacterial infections are biofilm based. Biofilms help to create multi-drug resistant (MDR) bacteria, which are becoming more common in healthcare.[8] Other biofilm bacteria that impact the economy through the food and water supply as well as transportation and shipping industries include *Escherichia coli, Listeria monocytogenes,* and *Salmonella typhi*.[9]

Biofilm is a structured community of bacterial cells enclosed in a self-produced polymeric, exopolysaccharide (EPS) matrix that adheres to an inert or living surface.[5,10,11] This EPS matrix is not solely structural, but also provides a protective aspect. Within the matrix, channels are formed for the transport of proteins and other nutrients to sustain of the viability of the bacterial colony. [7,11-16]The EPS is comprised of many different

macromolecules including proteins, nucleic acids, peptidoglycan, lipids, phospholipids, and even dead bacteria.[5,9,10,17-19] This structure is the basis for the protection of the

Table 1.1. Summary of biofilm producing bacteria with large impacts on human health.

Common bacterial biofilm species	Infection/disease	CDC threat level	Infections / Deaths per year	Comment
Methicillin-resistant *Staphylococcus aureus* (MRSA)	Nosocomial infection Medical implantable devices	Serious	80,461 / 11,285	Leading cause of healthcare-associated infections
Carbapenem-resistant *Enterobacteriaceae*	Biliary tract infection, Bacterial Prostatitis	Urgent	9,000 / 600	Has become resistant to nearly all available antibiotics
Streptococcus pneumoniae	Bacterial pneumonia and meningiti	Serious	1,200,000 / 7000	96 million in medical costs per year
Pseudomonas aeruginosa	Pneumonia, bloodstream, surgical site and urinary tract	Serious	51,000 / 440	6,700 infections are multidrug-resistant infections a year
Vancomycin-Resistant *Enterococcus*	Bloodstream, surgical site, urinary tract infections	Serious	66,000 / 1,300	20,000 drug resistant infections with few treatment options.
Drug-resistant *Salmonella typhi*	Typhoid fever	Serious	3800	21,700,000 infections worldwide 67% are drug resistant

bacterial colony from outside stressors, such as antibiotics, immune system responses of the host body, and also other bacteria.[9,18,20,21] Scheme 1.1 shows the primary events that lead to formation of biofilm and eventual spread of these bacterial infections.

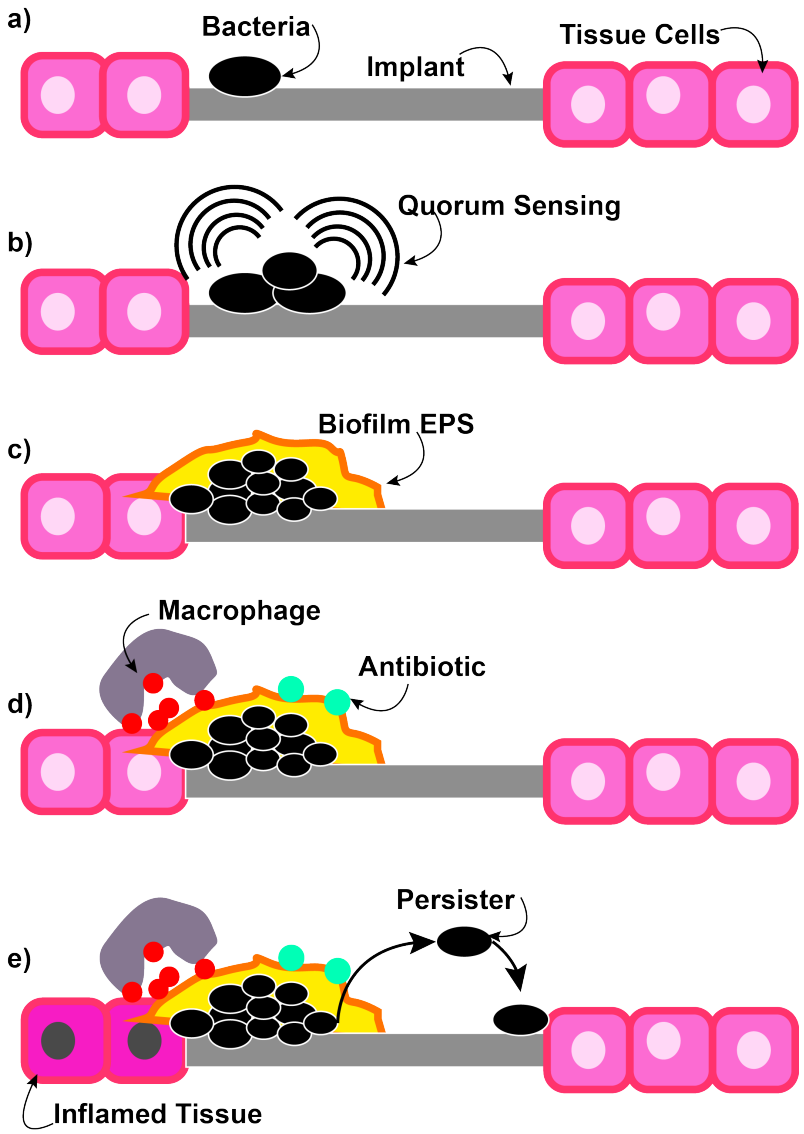

Scheme 1.1. Formation of biofilm. a) Planktonic bacteria settle on an adequate surface such as an implanted device in human tissue. b) Aggregation of the bacteria initiates QS, and c) biofilm EPS formation. d) Antibiotics and microphage processes cannot penetrate the biofilm resulting in e) inflamed tissue. Also, the biofilm can release persister cells that result in additional biofilm colonies.

As bacteria start to aggregate, they enter into a communication process called quorum sensing (QS) that allows for the coordination of the colony to form biofilm. QS is essentially influenced by a set of two proteins. One protein is responsible for the production of a signaling molecule, which is typically referred to as an autoinducer (AI), while the other protein responds to the AI. Once the AI have reached a critical threshold, the bacteria starts to produce biofilm.[11,22-25] The biofilm then works to attenuate the effectiveness of antibiotic processes to become a chronic infection essentially acting as a shield to protect against outside stressors, like antibiotics. Bacterial colonies that form biofilm have been found to be over 100 times less susceptible to antibiotics and disinfecting agents when compared to their non-biofilm counterparts.[2,7,16,23,25] This decrease is susceptibility is due to both tolerance and resistance. Tolerance is the process where bacteria do not grow but do not die, while resistance is the ability of bacteria to grow in the presence of a drug designed to kill it. All bacteria have the ability to become resistant to antibiotics regardless of their phenotype, but only bacterial colonies that form biofilm exhibit tolerance. [23,25]

Tolerance within the bacterial colony is based on the structure and the matrix composition. The EPS acts as a shield to stop the penetration of foreign agents deeper into the core of the colony.[2,25,26] The structure creates a layered environment where the core of the colony exists in a dormant state compared to the actively reproducing periphery. The dormant state works to minimize the effect of most antibiotics, which act by targeting metabolically active bacteria. The bulk of the bacterial colony exists in the dormant state until time comes for reproduction when persister cells are released.[16,23] Persister cells are bacterial cells that have attenuated metabolic and reproductive activity

and are highly tolerant to antibiotics. This tolerance is primarily because current antibiotic therapies target actively dividing cells. Overall, it is through the protective biofilm itself and the release of persister cells that these bacterial infections evade destruction via natural or pharmaceutical means. [3,7,12,23,27]

Anti-Biofilm Strategies

Biofilm-based bacteria are able to survive in hospital environments on tools and other non-biological instruments, evading eradication by cleaning agents such as triclosan, benalkonium chloride and chlorhexidine gluconate.[2] Many chronic infections start from bacteria surviving on surfaces such as implants or catheters. When these instruments and surfaces are used on or introduced to patients, bacteria may spread to the patients causing chronic infections.[1] The only way to remove biofilm infections is to remove the implant or infected tissue, which increases the risks of new infections and medical complications for the patient.[2,4,7,23,25] A chronic infection progresses slower than an acute infection. This slow development is what allows the bacteria to create a biofilm before any antibiotics are administered. Chronic infections can be treated with antibiotics, but it is very difficult.[2,4] Essentially the biofilm protects the underlying colony, the antibiotic is not effective at killing the dormant bacteria, and nutrient channels force the antibiotic out of the colony. Natural defenses only serve to enhance inflammation of the surrounding tissue by subjecting the biofilm to reactive oxygen species.[2,10,13,28] Also, only two new classes of antibiotics, oxazolidinones and lipopeptides, have been introduced into the clinic over the last 40 years. Oxazolidinones are broad spectrum antibiotics that inhibit protein synthesis by interfering with messenger RNA mechanisms.

Lipopeptides are antibiotics that disrupt several bacterial membrane functions, which causes an inhibition of protein, DNA and RNA synthesis.[29-31]

Studies of bacterial biofilms have shown that biofilms increase resistance to many antibiotics including ampicillin, tetracycline, penicillin, erythromycin, and chloramphenicol. However, the current treatment for biofilm infection is treatment of the infection with these broad spectrum antibiotics over several weeks, which is the same as for an acute infection.[6,9,22,23,27,32,33] This method may not successfully cure the infection. If a biofilm forms, then a persistent infection can occur leading to significant discomfort and prolonged illness. The methods currently used for suppressing or preventing bacterial biofilm formation are the early usage of antibiotics before biofilm can be formed, or the prolonged usage of antibiotics to suppress the bacteria once biofilm has been formed. Though both of these methods carry the risk of resistance being developed by the bacteria.[32,33] The most effective way to prevent a bacterial biofilm-based infection is to prevent the initial biofilm formation.

Based on the widespread health implications of biofilm, several antibiofilm antibiotic therapies have been proposed. Current promising methods for dealing with bacterial biofilm include the use of small molecules to control biofilm production. Small molecules such as autoinducing peptides, in addition to other signaling molecules, have been used to block bacterial signals that start production of biofilm within a colony. These molecules target the QS pathways described previously. Focusing on the AI pathway, promising therapies include acyl homoserine lactones (AHLs) to target Gram-negative bacteria and short peptides for Gram-positive bacteria. Overall, these studies essentially showed that small molecules that do not act as antibiotics or microbicides are

able to interfere with the regulatory systems that control biofilm formation and maintenance.[15,22,29,31] These small molecules can then be used in conjunction with established antibiotics to increase overall effectiveness of the antibacterial agents.

Another useful method for biofilm control is the use of natural products and natural product analogues. Plant extracts have been used in medicine for thousands of years. An example is traditional medicine, in which plant extracts and herbs are used, which continues to this day. Plants such as garlic and blackberries have been shown to possess compounds with antibiotic properties, and several studies have shown that biofilm colonies treated *in vitro* with these extracts were more susceptible to treatment with antibiotics. Natural products can sometimes exhibit less toxicity within the human body but also tend to be less effective than other methods.[17,29,31]

Antimicrobial peptides (AMP) have also been developed to control bacterial growth and biofilm formation. AMP are generally small, about 5-50 amino acid residues, and are highly positively charged.[8,30,34] They contain both a polar and non-polar regions as well as a well-defined regions of hydrophobicity and hydrophilicity. Since bacterial cells contain high percentages of negatively charged phospholipids, this allows for bonding of the AMP to the membrane. One major drawback to the existing AMPs is their degradation by enzymes, which limits their therapeutic effectiveness. AMP containing unnatural amino acids in their structure are promising as they are resistant to degradation in the human body, which allows them to more effectively penetrate the bacterial membrane and biofilm.[8,34] Theoretically, the unnatural AMP can create a path through or breakdown the biofilm, which in turn allows for the attack of antibiotics on the bacterial cells within the film. Also, based on the lack of degradation and lower amounts of

bioactivated metabolite species, they also exhibit lower toxicity compared to small molecules. AMP effectiveness is due to their mechanism of antimicrobial activity and the difficulty of bacteria to develop a resistance to them. AMP have been shown to play major roles in the defense mechanism and innate immune response for several living organisms against bacteria.[8]

A series of antimicrobial peptides (AMP) containing unnatural amino acids were synthesized and have been shown to be effective against several bacteria associated with chronic infection.[8] They were created to combat ESKAPE bacteria, which are known to commonly infect chronic wounds. These include *Enterococcus faecium* (meningitis), *Staphylococcus aureus* (boils, sinusitis), *Klebsiella pnemoniae (*pneumonia), *Acinetobacter baumannii* ("Iraqibacter"), *Pseudomonas aeruginosa* (opportunistic), and *Enterobacter* (opportunistic). The latter two are termed opportunistic pathogen in that they may lie dormant for periods of time in the body and cause little to no symptoms until overwhelming a compromised immune system that cannot raise adequate defenses. The AMP developed as potential agents against these bacteria contained unnatural amino acid dipeptide units tetrahydroisoquinolinecarboxylic acid (Tic) and octahydroindolecarboxyl acid (Oic). These Tic-Oic dipeptide units form a hydrophobic backbone and were coupled with cationic ammonium side chain groups that were connected to the main peptide sequence with varying carbon chain linkers.[8] A general structure of the unnatural amino acid containing AMP is shown below in Scheme 1.2, which also shows the Tic-Oic dipeptide structure. Due to the hydrophobic primary sequence interior, the peptide has been shown to primarily adopt an alpha helix structure.

In addition, these peptides were used against *solution phase,* or planktonic, bacteria from the aforementioned strains. Several of the AMP variants showed effectiveness in killing the bacteria in solution based on measuring cellular absorbance as the bacteria were exposed to the peptides. One peptide in particular, TTO-53 showed enhanced antimicrobial properties. TTO-53 is described in Chapter 2, while the three main peptides used in this particular study are also summarized in Scheme 1.2. Based on the effectiveness of the AMP toward the ESKAPE bacteria, we wanted to study these AMP for anti-biofilm activity, as this property has not yet been described for these peptides.[8] As stated previously, it is through the biofilm formation that these bacteria are so difficult to eradicate.

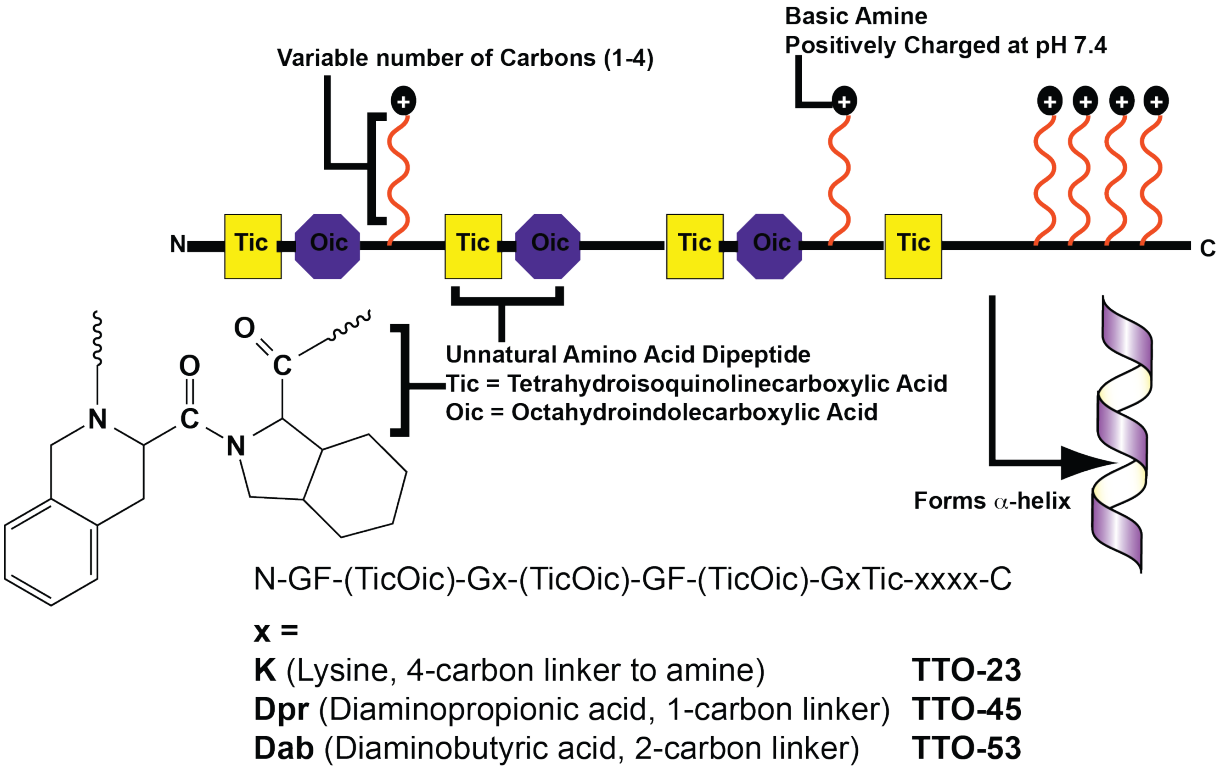

Scheme 1.2. General structure of the unnatural amino acid containing AMP used in this study.

Analysis Methods/Electrochemical Sensor Development

Currently, biological assays are the standard that is used to test the efficiency of antibiotics and antibiofilm agents. These assays include the introduction and exposure of the antibiotic or antibiofilm agent to a bacterial culture that is grown within the wells of a 96-well plate. The introduction of the antibacterial or anti-biofilm agent is done during the growth of the bacteria, an inhibition assay, or after the establishment of a biofilm on the walls of the plate, a dispersion assay.[7,32,35] In either case, the agent is allowed to interact over a timed period, usually 24 hours, and then compared to a control. This method allows for effective quantification of minimum inhibitory concentration (MIC) and also minimum bactericidal concentration (MBC). Both values are used to determine the viability of the agents against the tested bacterial strain. MIC is the lowest concentration of an antibacterial agent to inhibit growth. MBC is the lowest concentration of an antibacterial agent required to kill a particular bacterium. The testing can then be further analyzed through the use of dyes, such as crystal violet, and UV-Vis spectroscopy. Crystal violet dye can permeate the biofilm that is to be imaged. Later, the bound dye can be released via exposure to weak acid, and analyzed using visible spectroscopy. This allows the concentration of biofilm within each well to be quantified when compared by absorbance. Major issues with the current method are the amount of time required to perform a single test, which can span 1-2 weeks, cost of the instrumentation, and the volumes of solution needed. Larger volume amounts needed for well plate assays leads to high costs when employing unique small molecules or expensive synthesized peptides.

Electrochemical monitoring and sensor development have emerged as newer methods to determine the biological effectiveness of a variety of compounds. Electrochemical sensors offer speed, cost, and miniaturization benefits over standard assays. In addition, electrochemical sensors can offer answers to biological questions that take a fraction of the time compared to standard biological assays. Electrochemical methods include several different analysis techniques. Square wave voltammetry (SWV) and cyclic voltammetry (CV) are both highly utilized within electrochemical sensors. CV involves a linear increase and decrease of potential on a working electrode over time while monitoring the current. Current is then graphed vs. potential, which shows either diffusing or immobilized species reduced and oxidized at the electrode surface. CV provides directly quantitative information and also allows one to determine the redox potential of a species of interest. SWV offers enhanced sensitivity compared to CV. This technique differs from cyclic voltammetry in that it utilizes inputs of differential pulses as opposed to a linear sweep. The potential is pulsed forward and held for a period of time before being pulsed in the reverse direction and held again. The forward pulses increase several mV each subsequent cycle, which allows the potential to gradually become more positive or negative. The current is sampled twice during each cycle, once on the forward pulse and and once on the backward pulse, and the output is the difference in the current versus potential. The main advantage of SWV is the removal of charging currents via the pulse sequence, which means the output current is strictly Faradaic, or due to the studied redox process. Additionally, it is much faster than other derivative electrochemical methods. [20,24,36-38]

Several groups have utilized these techniques to develop electrochemical sensors to assay bacterial growth and breakdown. An electrochemical sensor was developed to quickly quantify the presence of certain bacterial species related to *P. aeruginosa*. This was through the detection of pyocyanin, which is produced by the bacteria. Pyocyanin gives the bacteria its blue-green color. Additionally, it plays a part in the QS mechanism of the bacteria colony while also acting as a toxin to fight off other bacteria. Studies using carbon fiber sensor assembly as combined detection element and transduction conduit were constructed to determine the concentration of pyocyanin in a system.[20,24] Rudimentary detection of pyocyanin in biological fluids has been studied before using a hanging mercury drop electrode (HMDE), but this method has not been used to detect pyocyanin in wound fluids. QS inhibition through pyocyanin detection has been seen using graphite rods as electrodes, relying upon differential pulse voltammetry (DPV). One of the main benefits of electrochemical biosensors is the ability for miniaturization. A miniaturized pyocyanin sensor was used to create a "smart-bandage," which, in theory, was able to provide intelligent *in situ* wound monitoring. This would allow for early detection of *P. aeruginosa* via pyocyanin production, which can then be treated before the biofilm can be fully established. The concentration of pyocyanin was detected down to 10 μM with variance of approximately 2%.[24]

Other studies focusing on the detection of *P. aeruginosa* via pyocyanin have utilized screen-printed electrodes and square wave voltammetry (SWV). Spiked urine sputum block and bronchial lavages were utilized to determine the detection limits of pyocyanin as an indicator of *P. aeruginosa*. The study was able to detect biologically relevant concentrations of pyocyanin, in the fluids spiked with *P. aeruginosa*, which

supported their hypothesis that electrochemical detection can be used to rapidly diagnose *P. aeruginosa* infections in biological fluids. These applications were both able to detect the presence of bacteria and show interactions within the bacterial system in a very rapid time frame.[20]

A multi-array electrochemical sensor with pattern recognition has shown usefulness in identifying bacteria based on antibiotic susceptibility. This study utilized the electrochemical sensor to measure the dissolved oxygen content in a 96-well plate. The study found that there was a steady decrease in dissolved oxygen as cells grew; however, in the presence of antibiotics at the MIC, no oxygen consumption was observed. This study showed that different types of bacteria can be identified using oxygen consumption curves, and the addition of antibiotics to the growth medium can then further increase the discrimination.[39]

While other studies have focused on detection of bacteria, we have developed an electrochemical sensor that seeks to mimic a standard biological biofilm assay where bacteria immobilized directly on an electrode surface can be monitored. Our studies here focused primarily on *P. aeruginosa*, for a multitude of reasons. It is a known biofilm producer, ease of biofilm growth, and its electrochemical activity.[7,20,23,40] The electrode biosensor was created using a layer-by-layer (LbL) method, which allowed the formation of a polymer bed on the electrode surface via subsequent and repeated exposure to polymers of opposite charge.[41-43] Once an underlying polymer surface was created, the final layers were formed based on how *P. aeruginosa* forms biofilms. We explored two avenues for the construction of the sensor. Our early efforts described in Chapter 3 focused on a more facile approach utilizing only the primary biofilm component

produced by *P. aeruginosa*, alginate. However, biological assay results described in Chapter 4 did not exactly match findings from the alginate electrochemical assay. Therefore, we explored ways to physically attach *P. aeruginosa* to the electrode surface in order to provide a more accurate sensor, which is described in Chapter 5. We show herein that this new electrochemical approach can provide an estimate of the antibiotic and anti-biofilm efficiency of a series of the aforementioned unnatural amino acid containing AMP toward *P. aeruginosa*. The sensor has the ability to evaluate anti-biofilm activity related to the AMP against *P. aeruginosa* in a significantly shorter time frame utilizing vastly reduced solution volumes of the AMP as compared to standard biological assays. Overall, the sensor technology described herein is a promising analytical method that may offer the ability to assay antibiofilm capabilities from a multitude of potential antibiotic drug candidates toward a variety of biofilm producing bacteria.

References

1. The direct medical costs of healthcare-associated infections in U.S. hospitals and the benefits of prevention - Scott_CostPaper.pdf. http://www.cdc.gov/HAI/pdfs/hai/Scott_CostPaper.pdf. Accessed 1/15/2015, 2015.

2. Costerton JW. Replacement of acute planctonic by chronic biofilm diseases. In The Biofilm Primer, Eckey, C., Ed., Springer: Berlin, 2007.

3. Costerton JW. Cystic fibrosis pathogenesis and the role of biofilms in persistent infection. *Trends Microbiol*. **2001**;*9*(2):50 - 52.

4. Costerton W, Veeh R, Shirtliff M, Pasmore M, Post C, Ehrlich G. The application of biofilm science to the study and control of chronic bacterial infections. *J. Clin. Invest*. **2003**;*112*(10):1466 -1477.

5. Jefferson KK. What drives bacteria to produce a biofilm? *FEMS Microbiol. Lett*. **2004**;*236*(2):163-173.

6. Donlan RM, Costerton JW. Biofilms: Survival mechanisms of clinically relevant microorganisms. *Clin. Microbiol. Rev*. **2002**;*15*(2):167-193.

7. Singh PK, Parsek MR, Greenberg EP, Welsh MJ. A component of innate immunity prevents bacterial biofilm development. *Nature*. **2002**;*417*(6888):552-555.

8. Hicks RP, Abercrombie JJ, Wong RK, Leung KP. *Bioorg. & Med. Chem.* **2012**;*21*:205.

9. Hall-Stoodley L, Costerton JW, Stoodley P. Bacterial biofilms: From the natural environment to infectious diseases. *Nat. Rev. Microbiol*. **2004**;*2*(2):95-108.

10. Hentzer M, Eberl L, Givskov M. Transcriptome analysis of pseudomonas aeruginosa biofilm development: Anaerobic respiration and iron limitation. *Biofilms*. **2005**;*2*(1):37-61.

11. Folsom JP, Richards L, Pitts B, et al. Physiology of pseudomonas aeruginosa in biofilms as revealed by transcriptome analysis. *BMC Microbiol*. **2010**;*10*, 294-2180-10-294.

12. Lewis K. Riddle of biofilm resistance. *Antimicrob. Agents Chemother*. **2001**;*45*(4):999 -1007.

13. Walters MC, Roe F, Bugnicourt A, Franklin MJ, Stewart PS. Contributions of antibiotic penetration, oxygen limitation, and low metabolic activity to tolerance of pseudomonas aeruginosa biofilms to ciprofloxacin and tobramycin. *Antimicrob. Agents Chemother*. **2003**;*47*(1):317-323.

14. Stewart PS. Mechanisms of antibiotic resistance in bacterial biofilms. *Int. J. Med. Microbiol*. **2002**;*292*(2):107-113.

15. Rogers SA, Huigens RW,3rd, Cavanagh J, Melander C. Synergistic effects between conventional antibiotics and 2-aminoimidazole-derived antibiofilm agents. *Antimicrob. Agents Chemother*. **2010**;*54*(5):2112-2118.

16. Kim J, Hahn JS, Franklin MJ, Stewart PS, Yoon J. Tolerance of dormant and active cells in pseudomonas aeruginosa PA01 biofilm to antimicrobial agents. *J Antimicrob Chemother*. **2009**;*63*(1):129-135.

17. Gaddy JA, Actis LA. Regulation of acinetobacter baumannii biofilm formation. *Future microbiol.* **2009**;*4*:273-278.

18. Stoodley P, Wilson S, Hall-Stoodley L, Boyle JD, Lappin-Scott HM, Costerton JW. Growth and detachment of cell clusters from mature mixed-species biofilms. *Appl Environ. Microbiol*. **2001**;*67*(12):5608-5613.

19. Sutherland I. The biofilm matrix – an immobilized but dynamic microbial environment. *Trends Microbiol*. **2001**;*9*(5):222-227.

20. Webster TA, Sismaet HJ, Conte JL, Chan IP, Goluch ED. Electrochemical detection of pseudomonas aeruginosa in human fluid samples via pyocyanin. *Biosens. Bioelectron*. **2014**;*60*:265-270.

21. Tenover FC. Mechanisms of antimicrobial resistance in bacteria. *Am. J. Med*. **2006**;*119*(6):S3- S10.

22. Geske GD, Wezeman RJ, Siegel AP, Blackwell HE. Small molecule inhibitors of bacterial quorum sensing and biofilm formation. *J. Am. Chem. Soc*. **2005**;*127*(37):12762-12763.

23. Hoiby N, Bjarnsholt T, Givskov M, Molin S, Ciofu O. Antibiotic resistance of bacterial biofilms. *Int. J. Antimicrob. Agents*. **2010**;*35*(4):322-332.

24. Sharp D, Gladstone P, Smith RB, Forsythe S, Davis J. Approaching intelligent infection diagnostics: Carbon fibre sensor for electrochemical pyocyanin detection. *Bioelectrochemistry*. **2010**;*77*(2):114-119.

25. Bjarnsholt T, Jensen PO, Burmolle M, et al. Pseudomonas aeruginosa tolerance to tobramycin, hydrogen peroxide and polymorphonuclear leukocytes is quorum-sensing dependent. *Microbiology*. **2005**;*151*(Pt 2):373-383.

26. Evans LR, Linker A. Production and characterization of the slime polysaccharide of pseudomonas aeruginosa. *J. Bacteriol*. **1973**;*116*(2):915-924.

27. Drenkard E, Ausubel FM. Pseudomonas biofilm formation and antibiotic resistance are linked to phenotypic variation. *Nature*. **2002**;*416*(6882):740-743.

28. Borriello G, Werner E, Roe F, Kim AM, Ehrlich GD, Stewart PS. Oxygen limitation contributes to antibiotic tolerance of pseudomonas aeruginosa in biofilms. *Antimicrob. Agents Chemother*. **2004**;*48*(7):2659-2664.

29. Worthington RJ, Richards JJ, Melander C. Small molecule control of bacterial biofilms. *Org. Biomol. Chem*. **2012**;*10*:7457.

30. Pigrau C, Almirante B. Oxazolidinones, glycopeptides and cyclic lipopeptides. *Enferm. Infecc. Microbiol. Clin*. **2009**;*27*(4):236-246.

31. Worthington RJ, Richards JJ, Melander C. Small molecule control of bacterial biofilms. *Org. Biomol. Chem*. **2012**;*10*(37):7457-7474.

32. Costerton JW. Bacterial biofilms: A common cause of persistent infection. *Science* **1999***; 284*, 1318.

33. Costerton, J. W., Lewandowski, Z., DeBeer, D., Caldwell, D., Korber, D., & James, G. Biofilms, the customized microniche. *J. Bacteriol*. **1994**;*176*(8):2137.

34. Russell AL, Kennedy AM, Spuches AM, Venugopal D, Bhonsle JB, Hicks RP. Spectroscopic and thermodynamic evidence for antimicrobial peptide membrane selectivity. *Chem. Phys. Lipids*. **2010**;*163*(6):488-497.

35. Stewart PS, William Costerton J. Antibiotic resistance of bacteria in biofilms. *The Lancet*. **2001**;*358*(9276):135-138.

36. Bogomolova A, Komarova E, Reber K, et al. Challenges of electrochemical impedance spectroscopy in protein biosensing. *Anal. Chem*. **2009**;*81*(10):3944-3949.

37. Baldrich E, Munoz FX, Garcia-Aljaro C. Electrochemical detection of quorum sensing signaling molecules by dual signal confirmation at microelectrode arrays. *Anal. Chem*. **2011**;*83*(6):2097-2103.

38. Hvastkovs EG, Buttry DA. Recent advances in electrochemical DNA hybridization sensors. *Analyst*. **2010**;*135*(8):1817-1829.

39. Karasinski J, White L, Zhang Y, et al. Detection and identification of bacteria using antibiotic susceptibility and a multi-array electrochemical sensor with pattern recognition. *Biosens. Bioelectron*. **2007**;*22*(11):2643-2649.

40. Wozniak DJ, Wyckoff TJ, Starkey M, et al. Alginate is not a significant component of the extracellular polysaccharide matrix of PA14 and PAO1 pseudomonas aeruginosa biofilms. *Proc Natl Acad Sci U S A*. **2003**;*100*(13):7907-7912.

41. Rusling JF, Hvastkovs EG, Hull DO, Schenkman JB. Biochemical applications of ultrathin films of enzymes, polyions and DNA. *Chem. Commun*. **2008**; 141-154.

42. Lvov YM, Lu Z, Schenkman JB, Zu X, Rusling JF. Direct electrochemistry of myoglobin and cytochrome P450cam in alternate layer-by-layer films with DNA and other polyions. *J. Am. Chem. Soc*. **1998**;*120*(17):4073-4080.

43. Borghol N, Mora L, Sakly N, et al. Electrochemical monitoring of chlorhexidine digluconate effect on polyelectrolyte immobilized bacteria and kinetic cell adhesion. *J. Biotechnol*. **2011**;*151*(1):114-121.

CHAPTER 2: EXPERIMENTAL

Electrochemical Assay

Materials

The peptides used in this study were synthesized in Prof. Rickey Hicks' lab following standard and reported protocols.[1] Additional TTO-53 was purchased from New England Peptide (Gardner, MA). The peptides had the general sequence:

N-GF-(TicOic)-Gx-(TicOic)-Gx-(TicOic)-GxTic-xxxx-C

Where is x =

K (lysine, 4-carbon linker to amine, TTO-23)

Dpr (diaminopropionic acid, 1-carbon linker, TTO-45)

Dab (diaminobutyric acid, 2-carbon linker, TTO-53)

Control Peptides

Control peptide 14 exhibits Tic-Oic units but does not contain any positive charges

Control peptide 34 only contains the cationic lysines.

The naming of the peptides denotes the number of Tic-Oic dipeptides in the sequence (T = tri, three) and the last number denotes a synthesis marker produced by the Hicks group at ECU. The peptides were delivered in previously lyophilized mg quantities. They were diluted in 10 mM Tris/10 mM NaCl pH 7.4 (E-buffer) to approximately 900 μM then

distributed into 100 μL aliquots. Before experiments, an aliquot was diluted with E-buffer to desired concentrations 0.1-25 μM.

Sodium alginate (Sigma Aldrich) solutions were created at approximately 3 mg mL^{-1} by mixing the alginate powder in E-buffer. After a short period to allow the alginate to solubilize, these solutions were used immediately.

Pseudomanas aeruginosa (strain PAO1) was obtained from Dr. Eric Anderson in the Department of Biology at East Carolina University. It was obtained from a glycerol stock and stored at -80^{o}C.

Tris(hydroxymethyl)amino methane buffer (Tris), potassium hexacyanoferrate (III) (ferricyanide, $Fe(CN)_6^{3-}$), poly(diallyldimethylammonium) chloride (PDDA), polystyrene sulfonate (PSS), and Luria broth mix (LB) were obtained from Sigma-Aldrich. All other materials were reagent grade and used as received.

Electrode film assembly

For the simplified alginate assay (Chapter 3), 2 mm-dia. pyroytic graphite (PG) electrodes were abraded on fine grit carbide paper and sonicated in water and ethanol followed by drying under a stream of argon. Layer by layer (LbL) films were formed on the electrodes by exposing the electrode to 30 μL drops of the following solutions for 15 min. each: PDDA, 2 mg mL^{-1} in deionized water + 50 mM NaCl, PSS, 2 mg mL^{-1} in deionized water + 50 mM NaCl, and alginate (3 mg mL^{-1} + 50 mM NaCl).[2] Electrodes were rinsed with deionized water between each layer. The final film formation was $(PDDA/PSS)_2PDDA/Alg$.

For the more detailed bacterial electrochemical assay (Chapter 5), electrodes were cleaned and prepared as described above followed by modifications with polymer and bacteria. The underlying polymer layers were PDDA/PSS/PDDA, which was then followed by exposure to the PAO1 bacteria. 1 mL of LB broth was inoculated with *P. aeruginosa* PAO1 using a sterile loop and allowed to grow overnight in a shaking incubator at 37^0C at 150 rpm. The bacteria was introduced onto the polymer-modified electrode surface by the addition of 10 μL of bacteria in LB broth solution directly to the electrode surface as a single drop. The electrodes were then capped and parafilmed to stop evaporation of bacteria solution from the electrode surface. The electrodes were placed into the incubator/shaker at 37 ^{0}C for a minimum of 6 hours and 50 rpm. Once complete, the final film formation was PDDA/PSS/PDDA/PAO1.

Electrochemistry

All electrochemical measurements were performed using a CH Instrument 660A work station. The modified electrodes were placed in an electrochemical cell containing 10 mL E-buffer along with a saturated calomel electrode (SCE) or Ag/AgCl (saturated KCl) reference electrode and a platinum wire as a counter electrode. Solutions were purged with Ar for 1 minute before each electrochemical run. For alginate films, cyclic voltammetry (CV) and square wave voltammetry (SWV) were employed to monitor the electrodes in the presence of 400 μM of $Fe(CN)_6^{3-}$. For PAO1 films, no ferricyanide was employed.

CV and SWV scans were taken initially before any exposure to AMP. This was the non-AMP exposure (t = 0 s) baseline. The electrode was then removed from the E-

buffer, rinsed briefly by submerging the electrode with a twisting motion in a solution of fresh E-buffer, and then exposed to 20 μL of the AMP. After the timed interval (15 – 600 s), the electrode was rinsed again with E-buffer, and placed back into the electrochemical analysis cell. CV was obtained at 100 mV s^{-1} scanning a complete from 0.5 V to 0.2 V forward scan and reversing back to 0.5 V, while SWV used the following parameters: potential range 0.5 to -0.2 V, step increment of 4 mV, amplitude of 25 mV, frequency 15 Hz, quiet time 2 s and sensitivity of $1x10^{-5}$ A.

Biological Assay

Materials

LB broth is comprised of the following 1.0% Tryptone, 0.5% Yeast Extract, 1.0% sodium chloride (NaCl) at a pH 7.0 The LB broth is created using the following parameters for 1 liter, the following chemicals were dissolved 10 g Tryptone, 5 g yeast extract, and 10 g NaCl in 950 ml deionized water. The pH of the solution was then adjusted to 7.0 with NaOH and the volume was brought up to 1 liter. The solution was then autoclaved.

LB Agar plates were created by preparing LB medium as above, but 15 g/L agar was added before autoclaving. After autoclaving, the solution was allowed to cool to approximately 55 ^{0}C, before being poured into 10 cm plates. The plates were allowed to solidify before they were inverted and stored at 4^{0}C.

Pirate growth media (pirate media) was created using 6 g Na_2HPO_4, 3 g KH_2PO_4, 0.5 g NaCl, 1 g NH_4Cl, 4 g arginine, and 1 liter of deionized water. The pH was adjusted

to 7.4 then autoclaved. Once cooled, 2 mL of 1 M $MgSO_4$ and 0.1 mL of 1 M $CaCl_2$ were added.

All other compounds were reagent grade and used as received.

Assay Procedure

Two biological assays were employed.[3,4] For the biofilm dispersion assay, LB broth 50 mL was inoculated with PAO1 using a sterile loop and allowed to grow overnight at 37°C in an incubating orbital shaker. The bacterial solution was then plated on the agar plates and again allowed to grow overnight at 37°C. Fresh LB medium was then inoculated with a single bacterial colony from the agar plate using a flame sterilized inoculating loop. Following the overnight growth, 100 μL of the bacteria was diluted 1:100 into pirate media. 100 μL of the PAO1/pirate media dilution was then added into each of the wells of a falcon brand flexible U-bottom 96 well-plate. The well-plate was then incubated overnight at 37°C on a shaker set at 250 rpm. Following the overnight growth, each well was then filled with 100 μL E-buffer containing peptide at desired μM concentrations. The plate was then allowed to react overnight in a shaker/incubator in the same manner as before.

For the inhibition biological assay, identical bacterial growth procedures were followed, but the peptides were then added into the bacteria/pirate media solution at the same time before reacting overnight in the shaker/incubator.

After incubation, the solution was discarded, and the microtiter plate was gently submerged in a small tub of water. The microtiter plate was filled with water and discarded several times. This rinsing step helps remove unattached cells and media components that can be stained in the next step, and significantly lowers background

staining. Crystal violet (125 μL, 0.1% in water) was added to each well of the microtiter plate, followed by incubating at room temperature for 10-15 min. The microtiter plate was then rinsed 3-4 times with water following the same protocol as outlined above. On the last rinse, the plate was blotted vigorously on a stack of paper towels to rid the plate of all excess cells and dye. The microtiter plate was then inverted and dried for a few hours or overnight. Once dry, the microtiter wells were photographed using a flatbed scanner.

UV-Vis Spectroscopy

To quantitatively measure the biofilm dispersion, 200 μL of 30% acetic acid were added to the wells to free the crystal violet from the film. The absorbance for each well at 540 nm was measured employing an Infinite M200 Pro multimode microplate reader.

Data Analysis

Data collected using the CHI interface were saved as .txt files and imported into Microsoft Excel. Columns could be manipulated in Excel and then it was imported into Origin Pro8 graphing software for further graphical analysis. Specifically, background plots were subtracted where 0s SWV runs of a particular AMP concentration series were subtracted from subsequent timed runs.

Images from the microtiter plate biological assay were imported into Adobe Photoshop for editing. Faux color was added to the images to demonstrate the biofilm density. The edited photos were then imported into Adobe Illustrator for further spatial manipulation.

References

1. Hicks RP, Abercrombie JJ, Wong RK, Leung KP. *Bioorg. Med. Chem*. **2012**;*21*:205.

2. Rusling JF, Hvastkovs EG, Hull DO, Schenkman JB. Biochemical applications of ultrathin films of enzymes, polyions and DNA. *Chem. Commun*. **2008**;141-154.

3. Evans LR, Linker A. Production and characterization of the slime polysaccharide of pseudomonas aeruginosa. *J. Bacteriol*. **1973**;*116*(2):915-924.

4. Hoiby N, Bjarnsholt T, Givskov M, Molin S, Ciofu O. Antibiotic resistance of bacterial biofilms. *Int. J. Antimicrob. Agents*. **2010**;*35*(4):322-332.

CHAPTER 3: LbL MODEL ALGINATE SENSOR

Results

Initial studies focused on developing a simple sensor designed to give a rapid answer to whether or not the Tic-Oic containing AMP were effective in penetrating biofilm. We were interested in testing the possibility that the AMP could penetrate a biofilm mimic, and that this penetration could be assayed electrochemically. Because certain biofilm can consist of polysaccharide films, layer by layer (LbL) electrode modification strategies were a natural choice to utilize in forming the electrodes.[1-3] Additionally, *Pseudomonas aeruginosa* is known to produce alginate containing biofilm; therefore, we focused on utilizing alginate in our films.[4,5]

LbL polymer films were formed by alternately exposing positive and negative

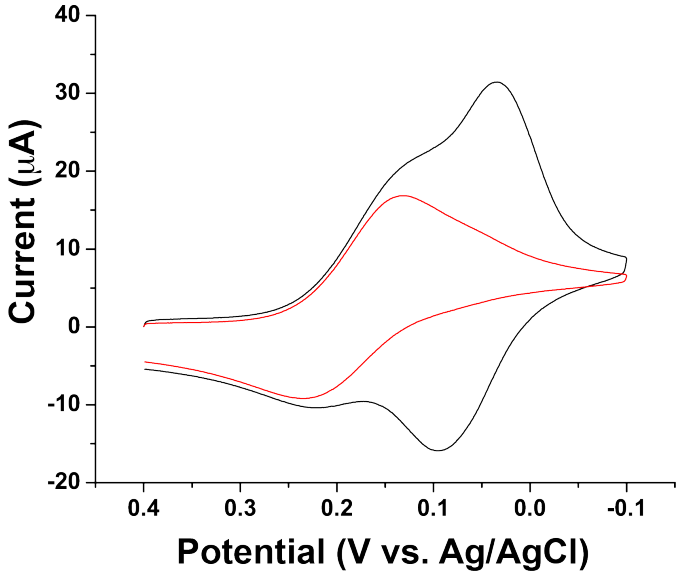

Figure 3.1. CV overlay showing the response of 400 μM ferricyanide at a PDDA/PSS/PDDA modified PG electrode (black) and a PDDA/PSS/PDDA/Alginate modified electrode (red). Conditions: E-buffer, pH 7.4, scan rate 100 mV/s.

charged polymers on a freshly prepared PG electrode, ending with the anionic alginate layer. The underlying layers act as a polymer "bed," and each subsequent polymer exposure essentially switches the surface charge of the electrode.[1] The films themselves are not electroactive; therefore, the films were monitored by probing the fate of a solution-phase redox active molecule, ferricyanide ($Fe(CN)_6^{3-}$). Initial studies were performed to demonstrate the presence of the alginate layer using cyclic voltammetry. This is shown in Figure 3.1. The CVs shows that ferricyanide will exhibit redox activity at two distinct potentials. The first location exhibits a formal redox potential at E^f at ~ +0.19V vs. Ag/AgCl. This is a classic diffusion-controlled process. The second, seen on the PG electrode without alginate in the black CV shows a E^f at +0.055 V vs. Ag/AgCl. This redox wave is more surface confined based on the ΔE_p of only 50 mV. The diffusive ferricyanide is also present at the non-alginate electrode as well. Addition of the anionic alginate layer to the underlying bed repels the solution phase anionic ferricyanide from binding to the electrode, forcing the redox process to occur via diffusion. The films are not sufficiently thick to eliminate this mode of electron transfer. When ferricyanide is not electrostatically repelled by the alginate, it binds to the cationic PDDA, and due to the electrostatic interaction, its oxidiative state is more stable by ~10 kJ/mol based on the 100 mV difference in redox potential between the two populations as shown in the relationship

$$\mathbf{\Delta G = -nFE} \qquad \mathbf{(3.1)}$$

where ΔG is the free energy change, n is the number of electrons (1), F is Faraday's constant (9.65×10^4 C mol^{-1}), and E is the reduction potential difference (0.1 V).

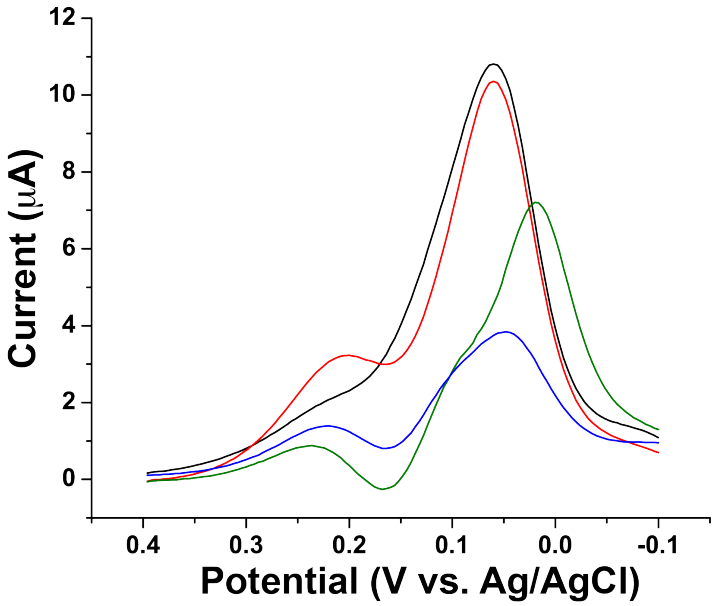

Figure 3.2. Background subtracted SWV overlay showing the response of 400 μM ferricyanide at an alginate modified electrode exposed to TTO-53 for 600 s. Electrodes were stored at 4°C for 5 hr (black) 24 hr (red) 48 hr (green) or 72 hr (blue) before use. Conditions: E-buffer, pH 7.4, SWV amplitude pulse 15 mV, step height 4 mV, f = 15 Hz.

After confirming the presence of the alginate layer, the films were exposed to solutions of the Tic-Oic AMP. This was performed by first obtaining a baseline SWV (or CV) in E-buffer, removing the electrode from that solution, applying a drop of the AMP containing solution to the electrode surface for a defined period of time, rising it off, and reinserting the electrode into the E-buffer. The purpose of obtaining the initial SWV was to background subtract subsequent timed runs from the baseline in order to see the current change as a function of AMP exposure. The first peptide to be tested was TTO-53, as this particular peptide was singled out in previous work as being particularly active toward the destruction of select ESKAPE bacteria.[6] Initial results were inconsistent, however, mainly due to the LbL formation protocols. Typically, LbL films can be

formed from stock polymer solutions and stored for prolonged periods with little impact to the resulting analytical signals. This is one of the key benefits of the modification procedure. In fact, LbL modified electrodes should sit for a time period (~24 hours) before electrochemical analysis, as it has been shown to improve the analytical results.[1,7] It became clear, however, that consistent results were only obtained by using fresh alginate solutions – i.e. made on the day of the electrode formation – and performing the electrochemical experiments within 24 hours of the electrode formation. Figure 3.2 shows the electrochemical response for alginate-modified electrodes stored for different periods of time exposed to TTO-53. The figure shows the background subtracted response, and current growth at the surface confined ferricyanide potential described in Figure 3.1. This will be discussed in more detail below; however, the change in current response was clearly more prevalent on electrodes analyzed within the 24-hr. window; therefore, analysis was performed on a consistent basis, allowing the electrodes to sit for 5 hours before performing experiments.

Following this regimented set of LbL-formation protocols, the complete series of AMP were studied to assess the possibility that they could disrupt the alginate layer. Figure 3.3 shows a typical example of this process employing 25 μM TTO-53 as the AMP. The figure first shows the raw SWV data for comparison purposes. The SWV of ferricyanide initially produces the single redox wave at the diffusion controlled potential, but after exposure to the AMP, the negative potential shifted peak grows in. This is consistent with easier access of the ferricyanide to the electrode surface as the electrode is exposed to TTO-53 for longer periods of time, which results in higher currents as this molecule is reduced at the electrode surface.

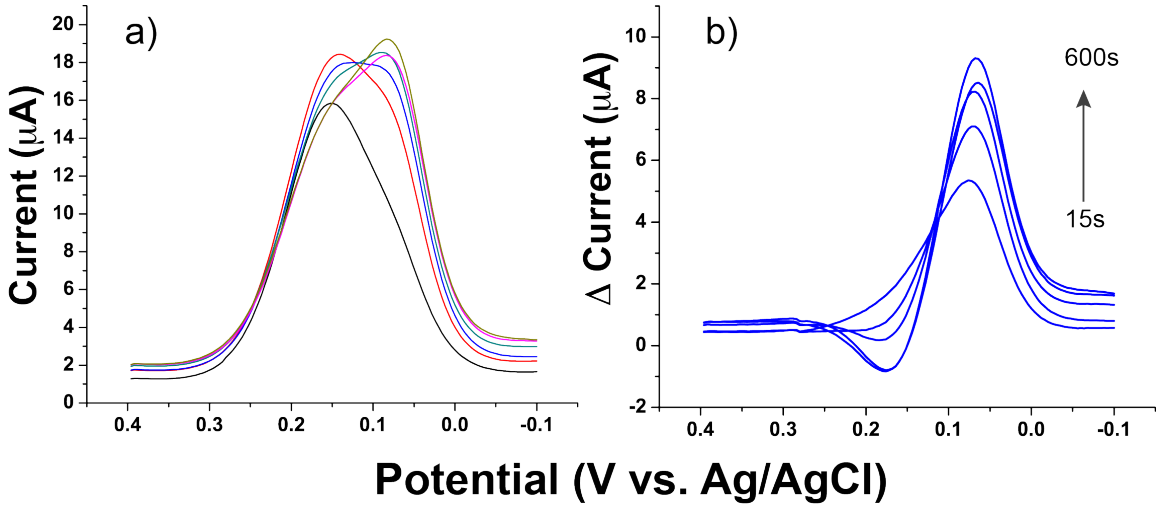

Figure 3.3. a) Raw SWV showing the response of 400 μM ferricyanide obtained at an alginate modified electrode exposed to 25 μM TTO-53 from 0s (black) to 600 s (mustard). b) Background subtracted SWV overlay obtained by subtracting the 0s SWV (black) from all subsequent SWV plots in a). Conditions: E-buffer, pH 7.4, SWV amplitude pulse 15 mV, step height 4 mV, f = 15 Hz.

Figure 3.3b shows the background subtracted SWV overlay where the 0s SWV was subtracted from the subsequent timed exposure runs. The differential plot provides a more convenient manner of showing that the ferricyanide population at +.075 V vs. Ag/AgCl emerges and grows with exposure to the AMP.

Figure 3.4 shows an overlay of the responses for TTO-23, 45, and 53 at 25 μM, as well as control responses for peptides 14 and 34. Peptide 14 contains three Tic-Oic residues, but does not contain the cationic tail, while Peptide 34 contains the lysine positive charged region, but is missing the Tic-Oic residues. The figure shows that TTO-23 was the most responsive toward alginate disruption causing higher ferricyanide

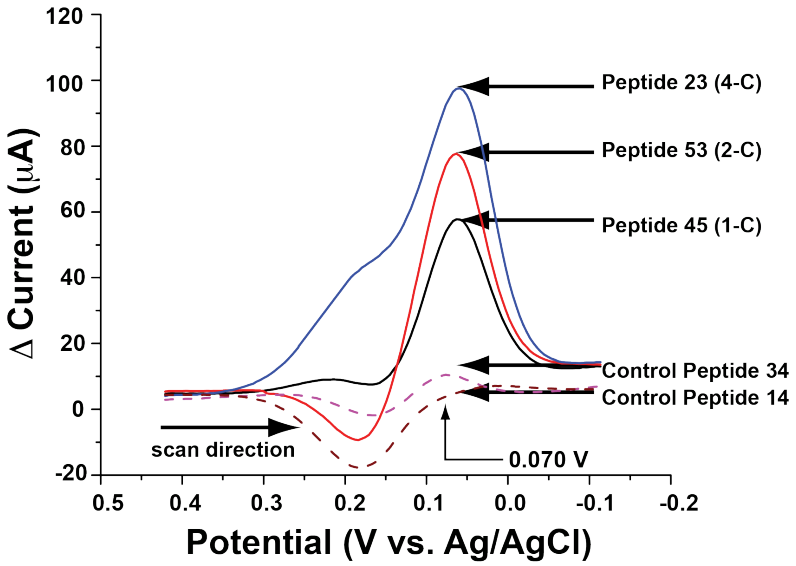

Figure 3.4. Background subtracted SWV showing the response of 400 μM ferricyanide obtained at an alginate-modified electrode at 300 s exposure to 25 μM TTO-23 (blue), TTO-53 (red), TTO-45 (black), Peptide 34 (dash purple), and Peptide 14 (dash dark maroon). Conditions: E-buffer, pH 7.4, SWV amplitude pulse 15 mV, step height 4 mV, f = 15

currents with time followed closely by TTO-53, and then TTO-45. The controls showed very little current change over the initial SWV background, and as such show almost a flat response upon exposure.

Figure 3.5 shows the time-dependent +0.070 V peak current response as a function of TTO-53 and TTO-23 concentration. The plot shows that the +0.070 V peak currents increase faster as a function of AMP concentration, which can be seen from the initial slope of the plots increasing as the concentration of TTO-53 or TTO-23 increases. Figure 3.6 shows the response for three TTO AMP at 25 μM. The figure also shows TTO-43, which is the peptide missing from the carbon-linker series that contains the three carbon linker to the ammonium. This peptide produced abnormal responses in many analyses (data not shown); however, and as such, this is the only data plot showing its response. The results show that TTO-23 was the most responsive, followed again by 53 and 45. Taken together, these data suggest that the breakdown of the alginate layer via exposure to the AMP is kinetically related to the following:

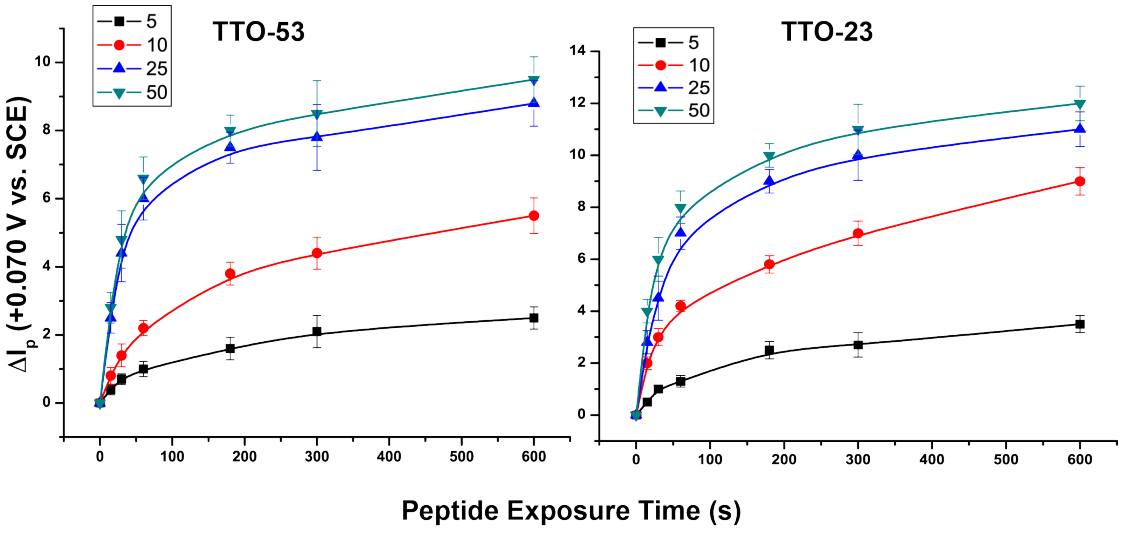

Figure 3.5. Change in SWV peak current vs. TTO-53 (left) and TTO-23 (right) exposure time for different μM AMP concentrations.

$$\text{Rate} = k'[\text{AMP}] \qquad (3.2)$$

Where AMP = the Tic-Oic peptide studied, and k' is the pseudo-first order rate constant.

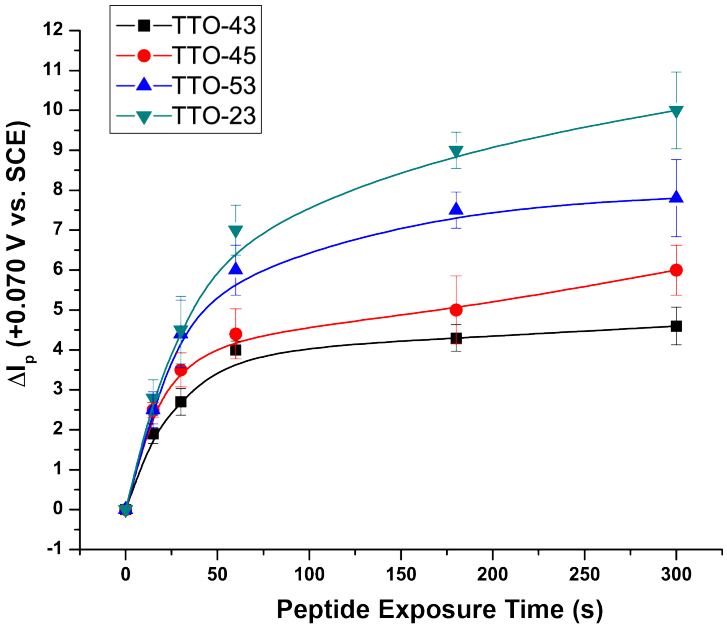

Figure 3.6. Change in SWV peak current vs. denoted AMP exposure at 25 μM concentration.

By taking the initial slopes of the plots shown in Figures 3.4-3.5, one can acquire the pseudo-first order rate constants for each of the peptides. These are summarized in Table 3.1. Overall, the data from Figures 3.5-3.6 and Table 3.1 show that TTO-23 was the most active toward alginate disruption causing increases in the +0.070 V ferricyanide peak current.

Table 3.1 Pseudo-first order rate constants for the AMP described in this study.[a]

TTO-53	3.7
TTO-23	4.5
TTO-45	2.9
TTO-43	2.7

[a] – nA μM^{-1} pepide s^{-1}

Discussion

The goal of this part of the sensor project was to generate a simple model to test the effectiveness of a series of AMP to penetrate a biofilm mimic. Alginate is the predominant biofilm compound produced by *Pseudomonas aeruginosa*, and as such was

a convenient polymer model employed and immobilized on the electrode using LbL methodology. Figure 3.1 clearly shows that alginate goes on the electrode, and provides a barrier to ferricyanide form accessing the underlying PDDA layer. When the ferricyanide can access the positively charged layer, it binds on the electrode surface electrostatically and generates a surface confined redox wave negative shifted from its diffusion redox wave.

Additionally, the alginate changes over time as shown in Figure 3.2. With time, the layers most likely swell due to the moisture on the electrode surface. This "matured" alginate layer is not as responsive to the AMP. Electrochemical responses were much lower for electrodes that had been allowed to sit for 3 days before exposure to AMP. Regardless, to obtain more consistent results, electrodes were used after allowing them to sit for 5 hours at 4^{o}C.

Figures 3.1-3.2 lay the foundation for the sensor responses seen when the alginate layers were exposed to the AMP. As the alginate was exposed to the AMP, ferricyanide can more easily access and bind to the electrode surface, as seen from peak current growth at +0.070 V over time (Figures 3.3-3.4). Peak growth at this potential is consistent with the breakdown of the alginate layer due to the AMP exposure and penetration of the outer alginate film, allowing ferricyanide to more easily access the electrode. Scheme 3.1 gives a pictorial overview of this process.

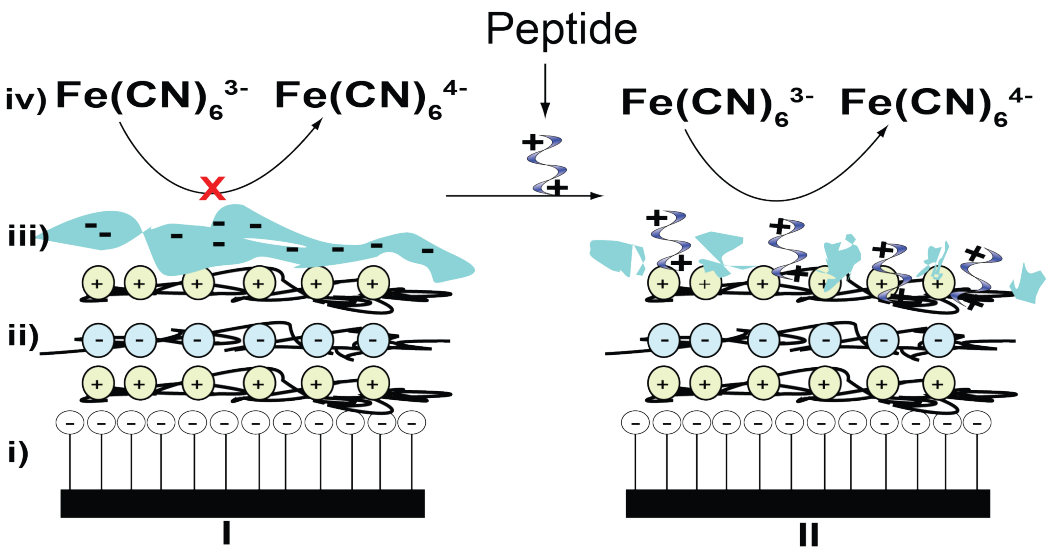

Scheme 3.1. I. The LbL electrode formed from i) a PG electrode, ii) inert polymers of opposite charge, and iii) alginate that prohibits iv) $Fe(CN)_6^{3-}$ from accessing the electrode. II. After peptide exposure, the alginate is broken penetrated, which allows $Fe(CN)_6^{3-}$ to access the electrode and produces higher electrochemical signals.

Current growth at the +0.070 V potential was shown to be dependent on both AMP concentration and identity. While all of the AMP (23, 45, and 53) all provided similar responses, TTO-23 was the most active, followed by 53, and then 45, which can be seen in Figure 3.6 and Table 3.1. From a trend perspective, this may be due to the length of the side chain linker that leads to the quaternized nitrogen on the AMP. TTO-23 contains a four carbon chain to a lysine, followed by a two carbon chain for TTO-53, and finally a one-carbon chain to the positively charge for TTO-45. The side chain linker may allow for easier initial access to the anionic alginate, which results in faster breakdown and ferricyanide access. However, the controls using Peptides 34 and 14 showed that the quaternized nitrogen cationic region was not sufficient by itself to breakdown the alginate. Peptide 34 contains the cationic lysine tail similar to TTO-23, but it exhibited very little response toward allowing ferricyanide to access the electrode.

This suggests two things: 1) the electrochemical response is due to the AMP opening up the alginate layer similar to what Scheme 3.1 depicts, and 2) the combination of Tic-Oic peptides as well as cationic charge are both necessary for this to occur. The second control peptide, Peptide 14, showed negligible activity toward the alginate layer. Peptide 14 contains Tic-Oic regions, but no cationic charge.

Overall, the LbL alginate model was effective in showing that the AMP could penetrate a biofilm mimic, and this process could be detected electrochemically. The electrode sensor showed that TTO-23 was the most active toward breaking down the alginate, followed by TTO-53 and then TTO-45. All of the peptides containing Tic-Oic dipeptide and cationic regions altered the alginate in such a way to generate a surface bound ferricyanide response. As discussed in Chapter 4 and 5, the elucidation that TTO-23 was the most active was not necessarily confirmed by other validation experiments. This is most likely due to the limitations of this simple sensor model. Some avenues for future studies include possibly studying how the AMP interact with the "mature" alginate layer (Figure 3.2) as this may change how each interacts altering the sensor output, which was not fully explored. However, the alginate sensor described here was incredibly easy to produce and had the ability to quickly identify peptides that were active in penetrating a biofilm mimic, and from this standpoint, the research presented here was a large success. This sensor could be thought of as a "first pass" type biofilm sensor, generating prospective "hits" that could be studied in more detail at later development stages.

References

1. Rusling JF, Hvastkovs EG, Hull DO, Schenkman JB. Biochemical applications of ultrathin films of enzymes, polyions and DNA. *Chem. Commun*. **2008**;141-154.

2. Costerton JW. Bacterial biofilms: A common cause of persistent infection. *Science* **1999***; 284, 1318*.

3. Costerton JW, Lewandowski Z, Caldwell DE, Korber DR, Lappin-Scott HM. Microbial biofilms. *Ann. Rev. Microbiol*. **1995**;*49*:711-745.

4. Evans LR, Linker A. Production and characterization of the slime polysaccharide of pseudomonas aeruginosa. *J. Bacteriol*. **1973**;*116*(2):915-924.

5. Sutherland I. The biofilm matrix – an immobilized but dynamic microbial environment. *Trends Microbiol*. **2001**;*9*(5):222-227.

6. Hicks RP, Abercrombie JJ, Wong RK, Leung KP. *Bioorg. Med. Chem*. **2012**;*21*:205.

7. Hvastkovs EG, Schenkman JB, Rusling JF. Metabolic toxicity screening using electrochemiluminescence arrays coupled with enzyme-DNA biocolloid reactors and liquid chromatography-mass spectrometry. *Ann. Rev. Anal. Chem*. **2012**;*5*:79-105.

CHAPTER 4: BIOLOGICAL ASSAYS

Results

After obtaining the results using the alginate LbL sensor, we explored ways to validate the results. The standard assay to test for anti-biofilm activity is to perform biological assays in 96-well or related plate formats. Here, two biological assays were performed. The first of these was a biofilm dispersion assay where *Pseudomanas aeruginosa* PAO1 was grown in the well plate under conditions that favor biofilm formation. The bacteria were diluted and stressed by placing them in what was termed "pirate media." This growth media is rich in arginine, hence the name. The media stresses the bacteria to initiate and establish biofilm on the sides of the well plate. After 24 hr growth period, the bacteria are removed and the AMP are introduced at sufficient volume to cover the biofilm level. The biofilm was exposed to the AMP for an additional 24 hr, and discarded. The remaining biofilm can then be stained using crystal violet, which penetrates and binds to the biofilm allowing it to be visualized. The more intense color means the higher amount of biofilm that was established or remains in the well.

Figure 4.1 shows the results of the biofilm dispersion assay where TTO-23, 45, and 53 at varying concentrations were exposed to the established PAO1 biofilm. The figure visually shows that all AMP showed some degree of biofilm dispersion, but TTO-53 was the most effective. Figure 4.1c shows the quantitative plate readout measuring A_{540} of free crystal violet released from the films. The plot shows that TTO-53 started to breakdown the biofilm at a concentration of about 1 μM, compared to approximately 10 μm for the other peptides. This was also seen in the qualitative top and side pictures of the assay.

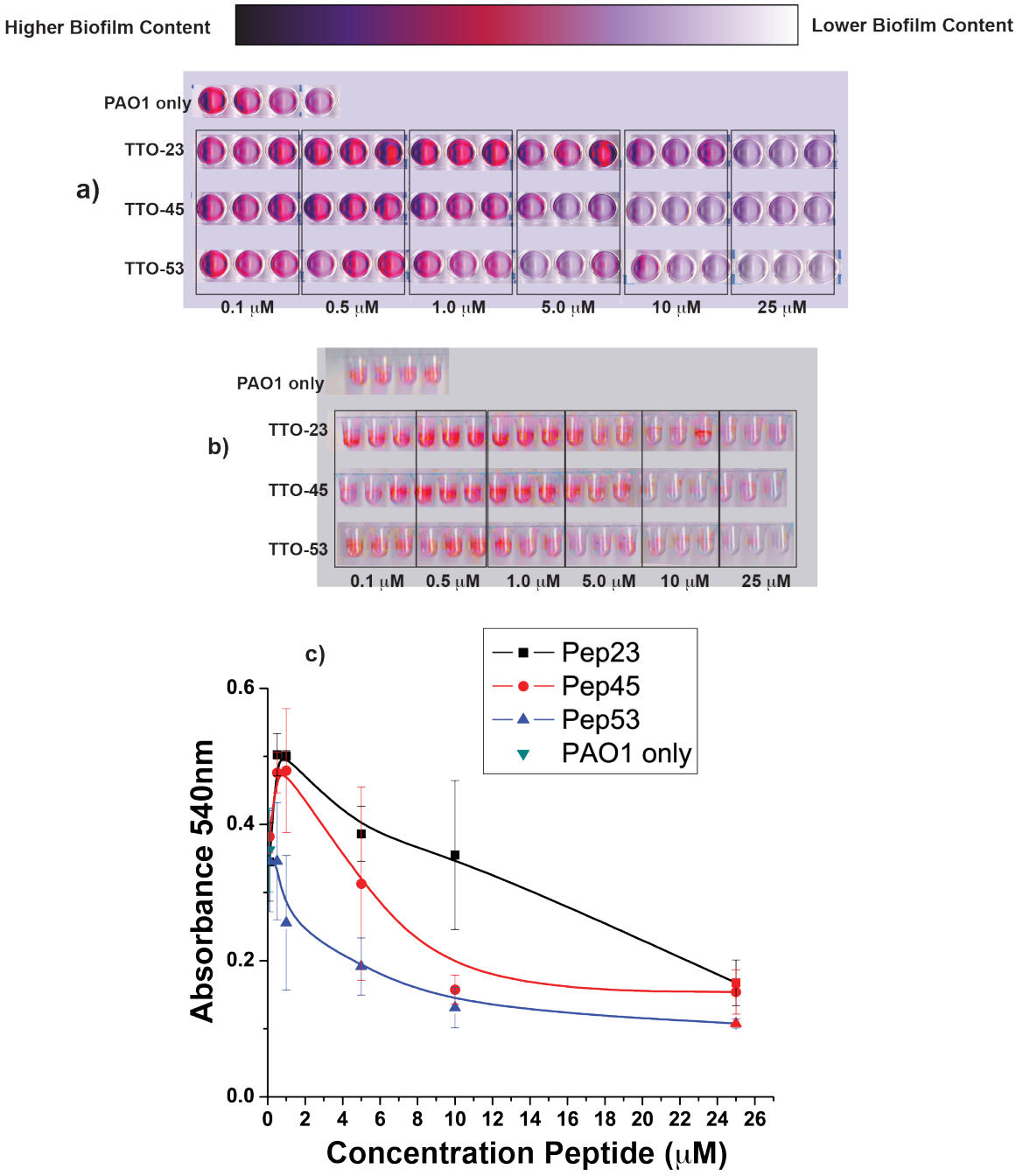

Figure 4.1. Top a) and side b) view of the dispersion assay where the denoted AMP were exposed to the established *Pseudomonas aeruginosa* PAO1 biofilm. Color was enhanced for visualization purposes and scale is shown. c) Quantification of the amount of crystal violet in the AMP-exposed wells measuring A_{540} vs. AMP concentration.

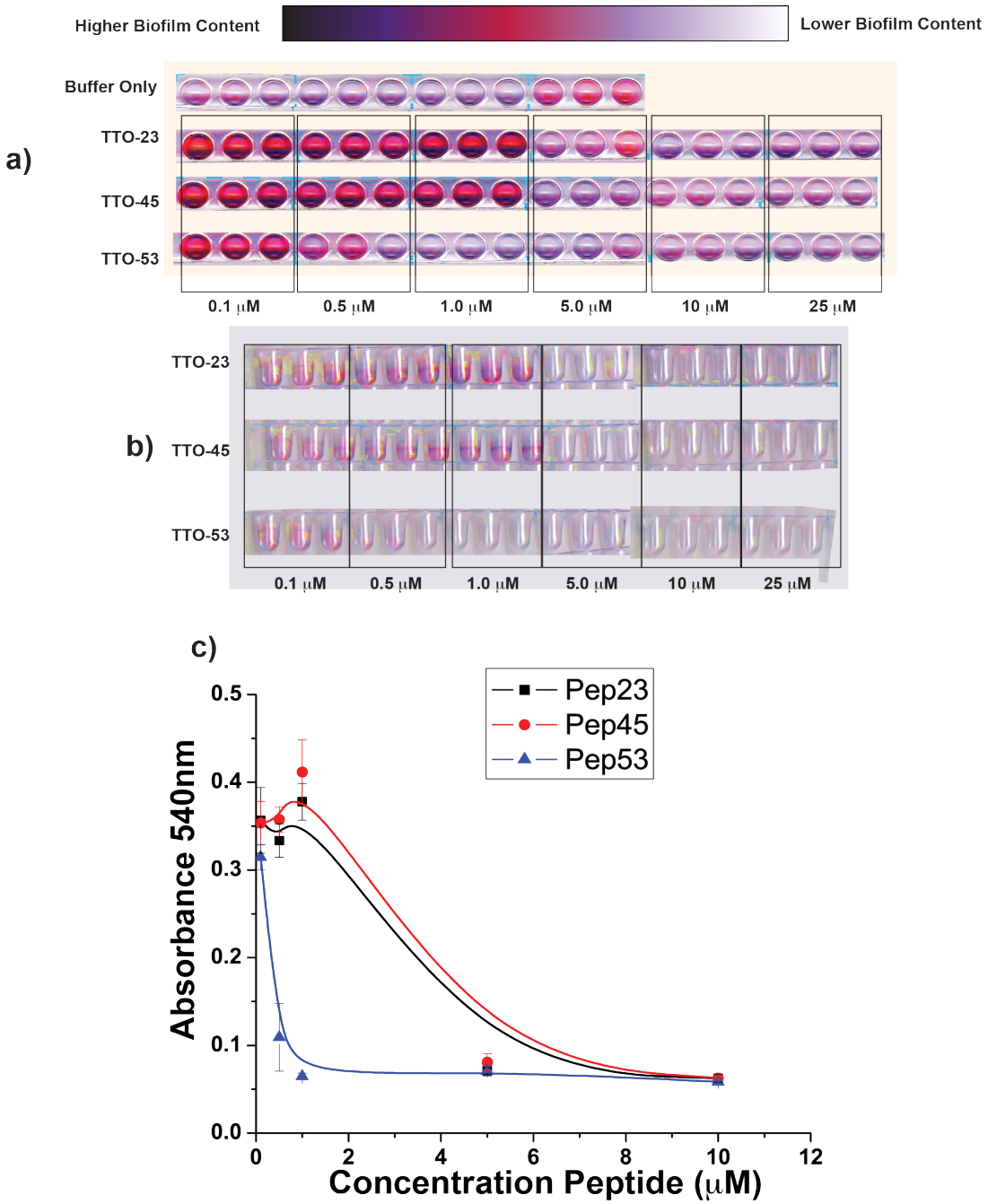

Figure 4.2. Top a) and side b) view of the inhibition assay where the denoted AMP were exposed to the *Pseudomonas aeruginosa* PAO1 solution concurrently. Color was enhanced for visualization purposes and scale is shown. c) Quantification of the amount of crystal violet in the AMP-exposed wells measuring A_{540} vs. AMP concentration.

Figure 4.2 shows the inhibition assay where the bacteria was grown concurrently with peptide exposure. This assay measures the ability of the AMP to inhibit bacterial growth and biofilm before it is established. The inhibition assay mirrored the dispersion assay results, but the AMP had much more of an impact inhibiting biofilm formation. This behavior was expected as these AMP had shown activity against planktonic *Pseudomonas* cultures.[1] Once again, all peptides inhibited bacterial growth, but TTO-53 was much more effective, inhibiting the biofilm at concentrations lower than 0.5 μM.

A control dispersion assay is shown in Figure 4.3. The figure shows that the control peptides 34 and 14 provided little anti-biofilm activity based on the similar color seen across the concentration range studied.

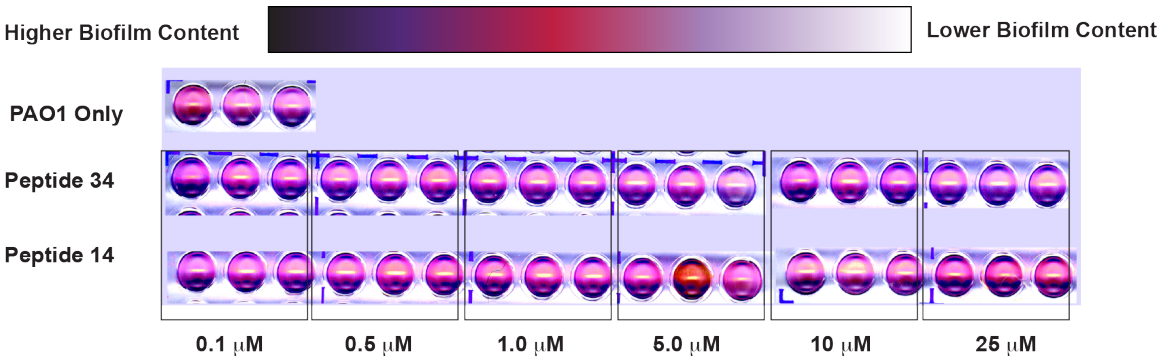

Figure 4.3. Top view of a dispersion assay where the denoted control peptide were exposed to the established *Pseudomonas aeruginosa* PAO1 biofilm. Color was enhanced for visualization purposes and scale is shown.

Discussion

The biological assay did not exactly agree with the preliminary electrochemical studies that showed that TTO-23 was the more effective AMP. Here TTO-53 was clearly the most effective AMP in precluding the biofilm from forming, but more importantly, dispersing established PAO1 biofilm. Based on previous results where these AMP were

exposed to the ESKAPE bacteria, these are not surprising findings. TTO-53 was shown to be more active toward bacterial killing based on in vitro susceptibility studies.[3] The MIC and MBC values across most of the six bacterial species showed slightly lower values when using TTO-53 when compared to TTO-23, showing greater effectiveness of TTO-53.

The data presented here is of high impact because it is the first example where these particular AMP were demonstrated to have anti-biofilm activity. While the alginate LbL model showed that these AMP could be active toward the breakdown of a protective barrier, these data definitively show that the biofilm is being either inhibited or destroyed by the AMP. Additionally, TTO-53 was a clear standout in terms of biofilm breakdown and inhibition, which provides additional support for its continued focus in the development as an antibacterial/anti-biofilm agent. Concerning these AMP and their anti-biofilm activity in general, this is somewhat surprising in that these peptides were designed to penetrate the anionic cell membrane of the actual bacteria, not necessarily breakdown established biofilm. Additionally, the controls show once again that it is the combination of the Tic-Oic units and the cationic charge that lead to effective biofilm disruption. Peptides 14 and 34 that exhibit only Tic-Oic units or cationic charge, respectively, showed essentially zero anti-biofilm activity.

The biological assay was explored to confirm, or validate, the electrochemical results, and while the agreement was not perfect, the discrepancies are not vastly different. The main similarities between the two assays was that both identified that the TTO AMP were effective in breaking down biofilm, and that the combination of the Tic-Oic residues plus cationic charge on the peptides was important. However, the order of

effectiveness was not the same for both assays. This main difference between the two methods is most likely due to the simplicity of the electrochemical model, which only highlights alginate penetration. As discussed previously, TTO-23 has a four-carbon linker to each ammonium group compared to TTO-53 that has a two-carbon linker. The four-carbon linker of TTO-23 may enhance alginate breakdown but not assist in killing the underlying bacteria at the lower concentrations where TTO-53 was more effective.

In vivo, biofilm is created from the genetic material found within the bacterial colonies; therefore, different bacteria will produce a unique bacterial biofilm. Therefore, while alginate provides a decent model to study the possibility of the AMP anti-biofilm activity, or in theory any potential anti-biofilm agent, toward *P. aeruginosa,* the actual situation is much more complex in scope. As the biological assays demonstrated, the simplicity of the alginate model leads to its main drawback in that it can identify a series of anti-biofilm agents, but can't accurately provide which agent exhibits the most anti-biofilm activity. In order to reconcile these main differences, the biological assay and the alginate model were essentially combined onto an electrochemical interface, which is discussed further in Chapter 5.

References

1. Hicks RP, Abercrombie JJ, Wong RK, Leung KP. *Bioorg. Med. Chem*. **2012**;*21*:205.

CHAPTER 5: ANTI-BIOFILM ELECTROCHEMICAL SENSOR WITH IMMOBILIZED BACTERIA

In order to reconcile the biological data (Chapter 4) and the electrochemical sensor data (Chapter 3), the development of a more biologically accurate sensor was explored. We desired the simplicity of our original sensor, but also to immobilize actual biofilm-forming bacteria on the electrode surface. The original plan was to grow *Pseudomonas aeruginosa* on the electrode surfaces in a similar way as was performed for the biological assays, using Pirate media to induce biofilm production. Following the bacteria growth on the electrode, similar protocols as were implemented for the alginate sensor would be utilized – i.e. electrochemical detection of ferricyanide while exposing

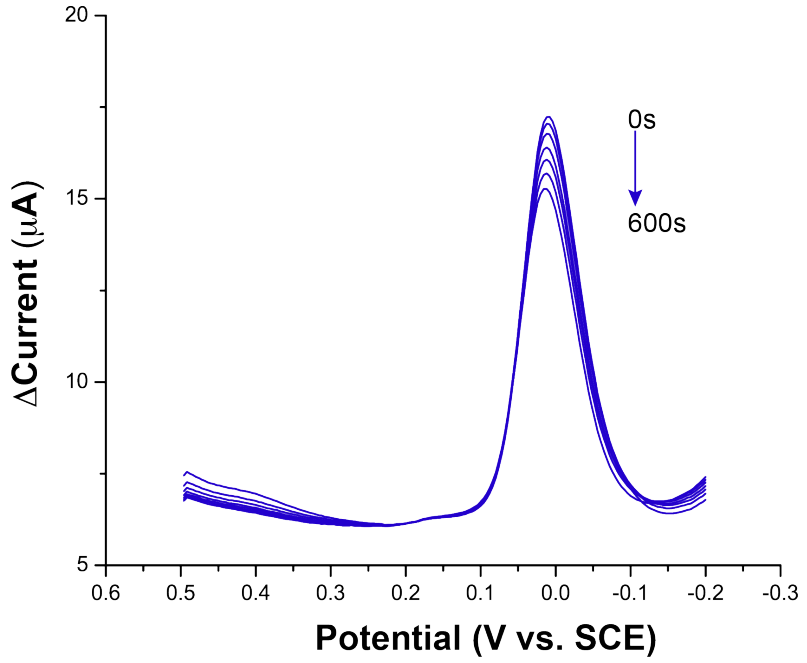

Figure 5.1. SWV showing timed response of *P. aeruginosa* PAO1 modified electrode exposed to only E-buffer from 0 s to 600 s. SWV Conditions: 20 mV pulse height, 4 mV step height, 15 Hz frequency, E-buffer pH 7.4.

the surface to the AMP. Initial results were inconsistent, and it was clear that growing the bacteria on the electrode in this fashion was untenable.

To remedy these drawbacks, a simpler method was utilized. This involved growing the PAO1 in LB broth for a period of time until it was visually clear that the bacteria were inducing the QS pathways needed for biofilm production. This is evident from the green color that is generated from expressed pyocyanin, which is discussed further below. Once the bacteria produced suitable biofilm, an aliquot of LB broth was exposed directly to the PDDA/PSS/PDDA modified electrode surface. The bacteria solution was then allowed to immobilize for a period of time. This immobilization time turned out to be a vital aspect in the sensor design. Figure 5.1 shows the SWV electrochemical response for an electrode modified with *P. aeruginosa* for 6 hours. The figure shows two important things. First, the bacteria itself is electroactive, which negates the need to include ferricyanide as a secondary solution-phase redox mediator. The redox active nature of *P. aeruginosa* arises from the expressed pyocyanin, which it releases as it forms biofilm. The reduction peak at +0.030 V vs. Ag/AgCl is not as negative as pure pyocyanin immobilized on the electrode, and the reasons are discussed later (see below), which may result from the electrode environment including pH effects and other binding environments based on the LbL/bacterial nature of the film.[1] Second, the SWV peak decreases slightly over the ten-minute analysis time, which is somewhat problematic, but manageable, as later results will show. The decrease in peak current is consistent with loss of bacteria over time, or rearrangement of the film on the electrode surface over that time; however, it provides a useful electrochemical signal to probe the fate of the bacteria.

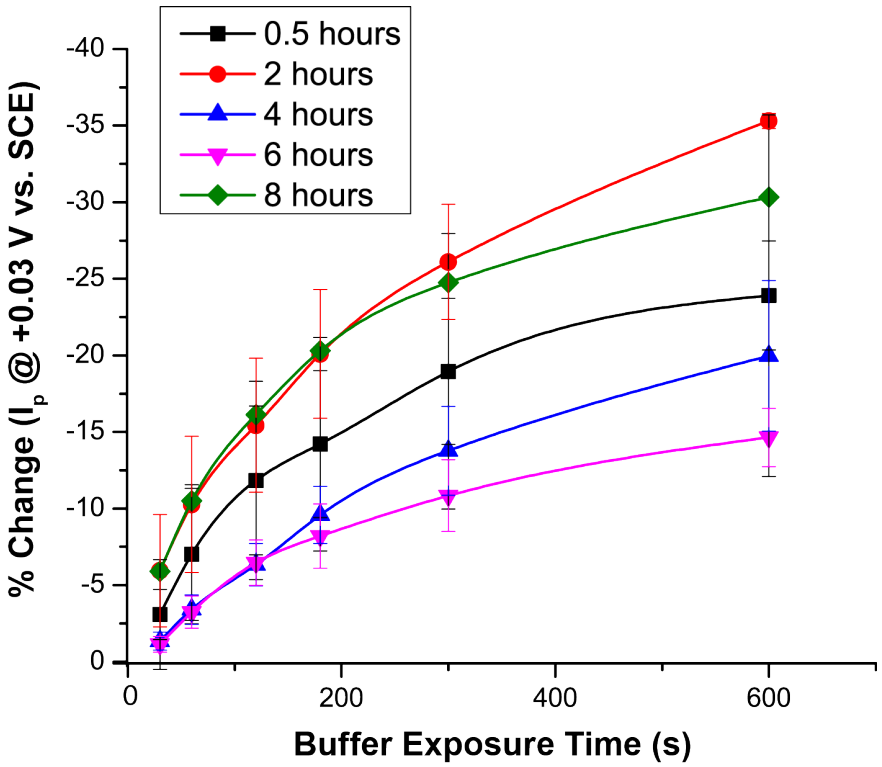

Figure 5.2. Percent change of peak SWV current at +0.03 V vs. SCE for *P. aeruginosa* PAO1 modified electrodes. Bacteria was allowed to immobilize on electrode for denoted amounts of time. Error bars represent standard deviation for n = 3.

Figure 5.2 shows the +0.030 V SWV peak current results over time for different electrodes modified in the same way, but allowing the bacteria to immobilize for the denoted period of time before placing the electrode in E-buffer. The figure shows that the bacteria was least resistant to change on electrodes where it was allowed to immobilize for 6 hours. The exact reasons for this are not fully understood at this time, but may include the conditions that the bacteria are exposed to on the electrode surface. For instance, ionic strength conditions may be affecting the viability of the bacteria, causing the peak decrease over time. This possibility was not tested further. However, the percent change at 6 hours was deemed satisfactory, and based on these results, *P.*

aeruginosa was allowed to immobilize on the electrode surface for 6 hours for the AMP experiments described below.

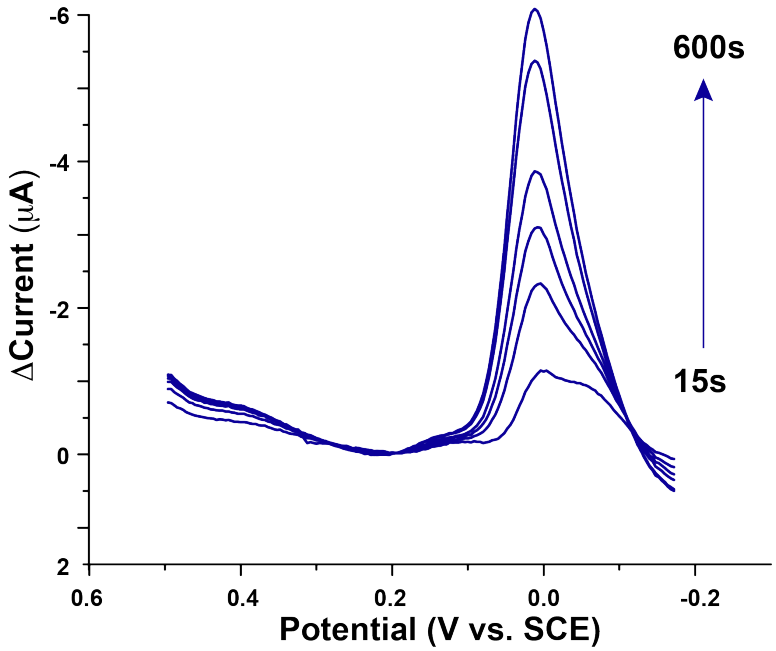

Figure 5.3. Background subtracted SWV showing timed response of *P. aeruginosa* PAO1 modified electrode exposed to 0.1 μM TTO-53 from 15 s to 600 s. SWV Conditions: 20 mV pulse height, 4 mV step height, 15 Hz frequency, E-buffer pH 7.4.

Figure 5.3 shows the typical *P. aeruginosa* electrochemical reduction response over time as it was exposed to 0.1 μM TTO-53. The figure shows a background subtracted then inverted plot that resembles peak growth, but the raw data plot is actually a peak decrease, which is seen looking at the y-axis showing current decrease. The plot shows that exposure to TTO-53 results in a significant PAO1 peak decrease over the exposed time. The current decrease at the final ten minute acquisition time corresponds to over 40% signal decrease from the initial peak obtained at the 0s exposure time. This

shows that the exposure to the AMP results in significantly more current change vs. exposure to buffer alone (Figure 5.1).

Figure 5.4 shows the peak current change responses for all peptides at 0.5 μM exposed to the *Pseudomonas* modified electrodes at 300 s. The figure demonstrates that TTO-53 is much more active in promoting change to the bacteria at this lower concentrations than the other AMP. The figure shows that the control peptides are slightly less active than the other AMP, TTO-23 and TTO-45, but only slightly at this low concentration.

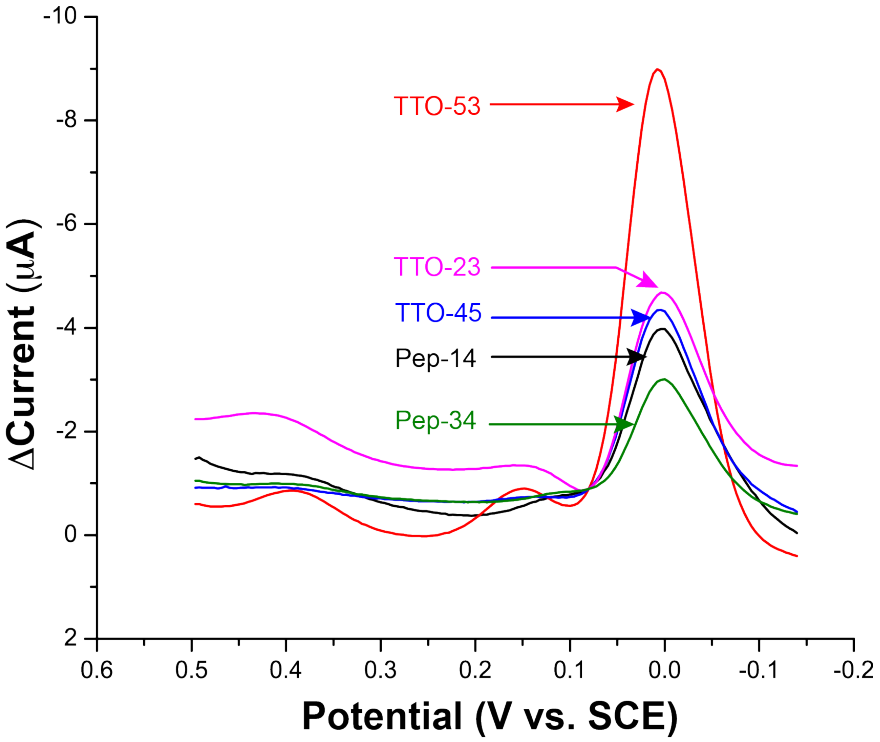

Figure 5.4. Background subtracted SWV showing response of *P. aeruginosa* PAO1 modified electrodes exposed to the denoted peptides at 0.5 μM for 300s. Conditions: SWV amplitude pulse 20 mV, step height 4 mV, 15 Hz, E-buffer pH 7.4.

TTO-53 was much more active toward decreasing the electrochemical PAO1 signal at lower concentrations vs. the other peptides. A plot showing the background subtracted peak current percent change at +0.03 V vs. TTO-53 exposure time for the entire studied concentration range is shown in Figure 5.5. The figure shows that this particular peptide was very effective toward altering the *Pseudomonas* electrochemistry

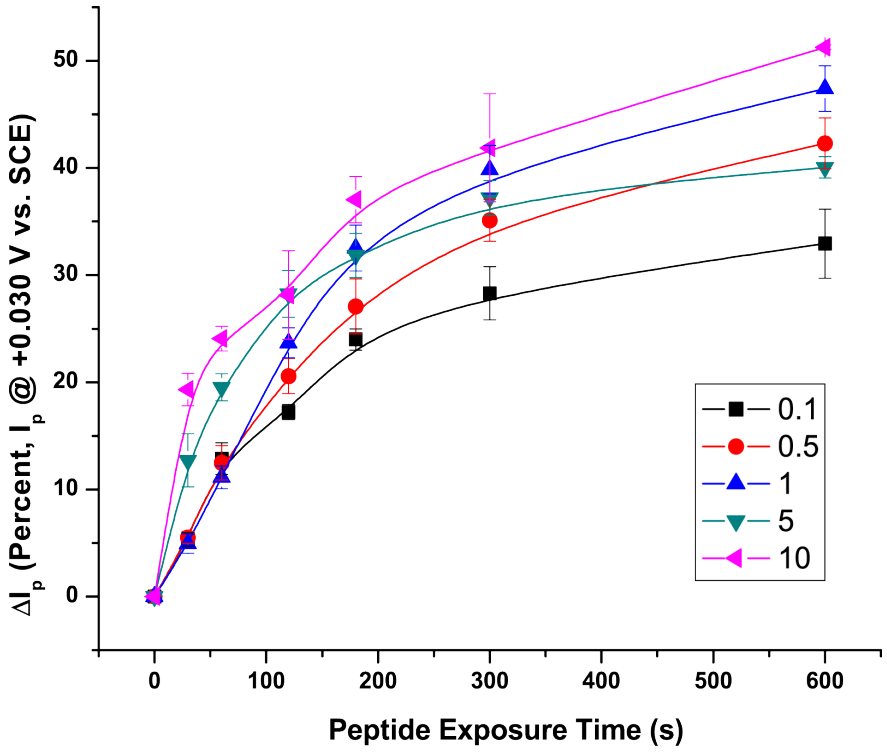

Figure 5.5. +0.03 V SWV I_p vs. TTO-53 exposure time at different concentrations in μM. Error bars are for standard deviation (n = 3).

at lower concentrations, but this behavior was not as prominent at higher concentrations, as the response increased, but only slightly. Other peptides, however, were much more

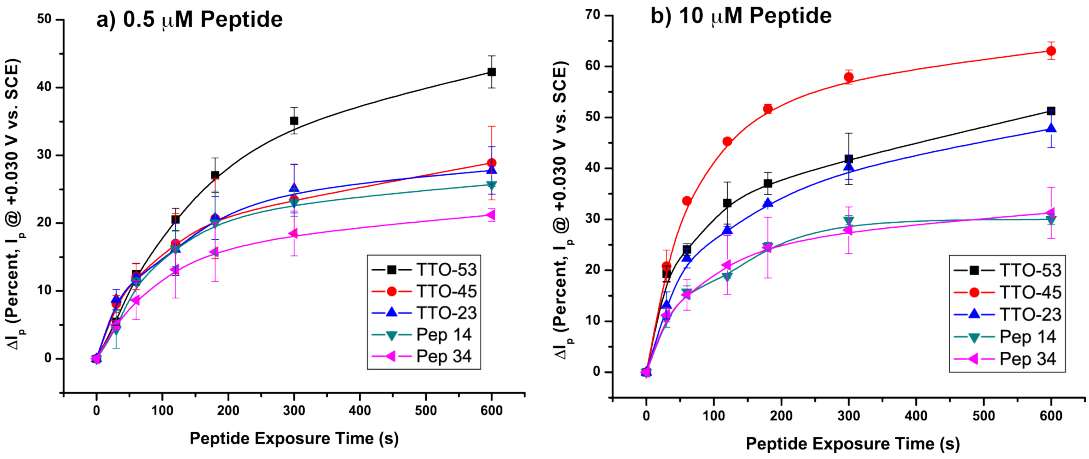

Figure 5.6. a) +0.03 V SWV I_p percent change decrease vs. peptide exposure time for all peptides at 0.5 μM. b) The same plot for for peptides at 10 μM. at different concentrations.

active toward altering the *Pseudomonas* electrochemical behavior at higher concentrations. A similar kinetic plot showing the response of all peptides at 0.5 μM and 10 μM is shown in Figure 5.6 a-b. Figure 5.6a shows that at the lower concentration, TTO-53 exhibited the most response, but at higher concentrations, TTO-45 was the most active. All TTO AMP exhibited higher responses than the controls. Also, it is important to remember that the responses seen here also include some current change from the bacteria by itself (Figure 5.1-5.2). However, at 5-10 minutes the percent change from that process amounted to approximately 10-13% of the current loss. Therefore, after accounting for this current, the AMP peptides are actually much more active toward altering the *Pseudomonas* on the electrode surface than the control peptides were.

The kinetic plots showing the response at different concentrations for the various AMP and control peptides were used to generate pseudo-first order kinetic rate constants for the different peptides exposed to *Pseudomonas*. These data are summarized as relative values in Table 5.1 for the different high and low concentration ranges. The data are presented in this manner, as there was a clear change in behavior for the peptides as the concentration of peptide increased. The table shows that the AMP were up to five-times more active in affecting *Pseudomonas* electrochemistry compared to the control peptides. This was even more evident at the higher concentration ranges.

Table 5.1. Relative kinetic rates determined electrochemically for different TTO AMP toward *Pseudomonas aeruginosa* PAO1 breakdown.[a]

Peptide	**< 1 μM**	**> 1 μM**
TTO-53	1	0.61
TTO-45	0.62	1
TTO-23	0.56	0.45
Peptide 14	0.43	0.27
Peptide 34	0.27	0.28

[a] - Adjusted for current change due to E-buffer alone

Discussion

Pseudomonas aeruginosa was successfully immobilized on the PG-electrodes in order to create a biofilm sensor. Data presented in Figure 5.1 show that a clear electrochemical signal is seen after exposure of the electrode to the bacteria, which means that this signal is clearly due to its presence on the electrode surface. Exposure of the

bacteria-modified electrode resulted in a decrease in the bacteria-related current. This is shown in Figures 5.3 and 5.4 where the background subtracted SWV denote current *decrease*.

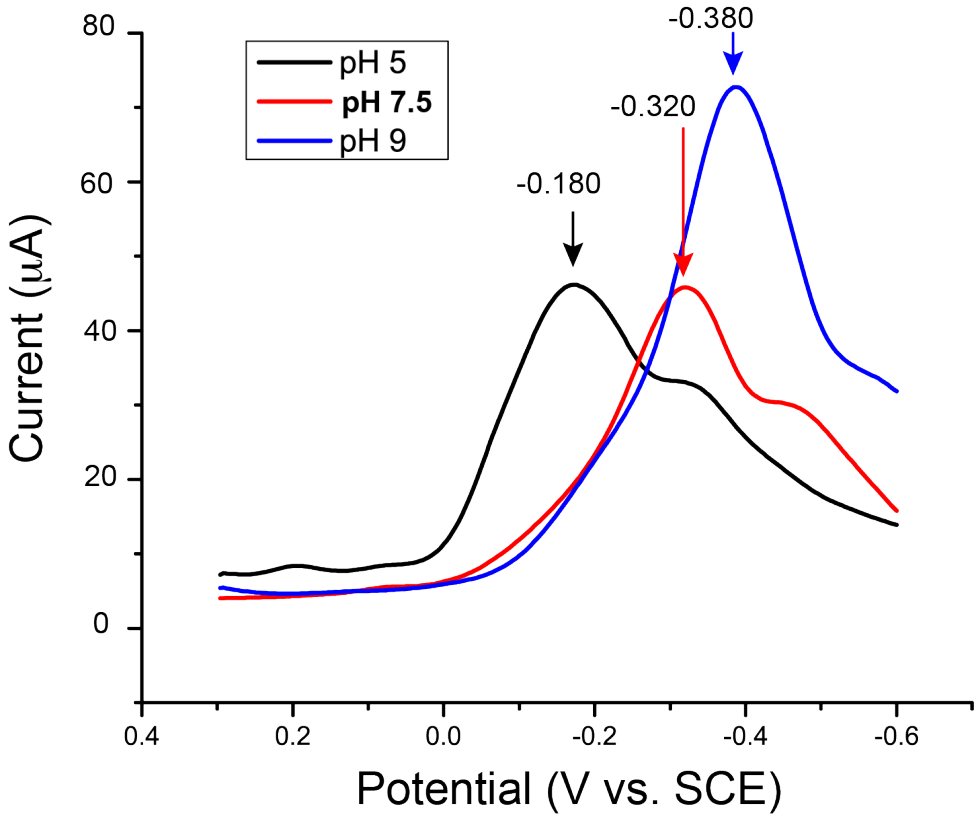

Figure 5.7. SWV response for pyocyanin modified electrode in different pH buffers. Conditions: SWV peak amplitude 20 mV, step heigh 4 mV, 15 Hz. pH 5 buffer = ammonium acetate 50 mM, pH 7.5 and 9 buffer: 10 mM Tris + 10 mM NaCl pH adjusted.

Previous data presented in Chapters 3 showed that the AMP would affect electrochemical signals on an alginate-modified electrode, but that TTO-23 was the most effective, followed closely by TTP-53. The biological assay presented in Chapter 4 showed that TTO-53 was the most effective AMP in treating biofilm. Data presented here are more consistent with the biological response data of Chapter 4. At low

concentrations, i.e. below 1 μM peptide, the electrochemical change based on peptide exposure is higher for TTO-53 compared to the other peptides. At higher concentrations, the other AMP become more effective in altering the electrochemical signals, and this was again seen in the biological assay where the biofilm was destroyed with these AMP at the higher concentrations.

Concerning the electrochemical signal, it is most likely the electrochemical response of pyocyanin within the bacterial colonies that are immobilized on the electrode surface. Figure 5.7 shows the electrochemical response of isolated pyocyanin immobilized on a bare PG electrode at different pH. The responses seen in the figure are much more negative shifted compared to what was seen for the bacteria response like that shown in Figure 5.1. The reasons for this potential difference could be the environment that the pyocyanin exists in while in the bacteria vs. isolated. The figure shows that a clear pH dependence exists, which is indicative of a proton-coupled electron transfer process in the reduction of the molecule. It is possible that the pyocyanin resides in an environment while immobilized in the LbL films that facilitates the proton coupled electron transfer resulting in the destabilization of the oxidized pyocyanin species and promotes the reduction at significantly positive shifted potentials. More experiments are needed to fully understand this process.

What is understood, however, is that upon exposure to the AMP, the pyocyanin-related electrochemical peak from the *P. aeruginosa* decreases. This decrease is consistent with some alteration of the bacterial environment on the electrode surface. This could be due to bacterial death or film modification due to the peptide exposure. Scheme 5.1 graphically demonstrates this process on the electrode. These AMP have

been known to penetrate and aggregate within bacterial membranes based on the cationic charge that they exhibit, essentially resulting in bacterial lysis.[2] This ability to utilize the cationic nature to bind to a surface was the main reason for the use of the anionic alginate model described in Chapter 3. A similar process could be occurring here where the AMP initially bind, then aggregate to promote bacterial film breakdown and promote the death of the bacteria.

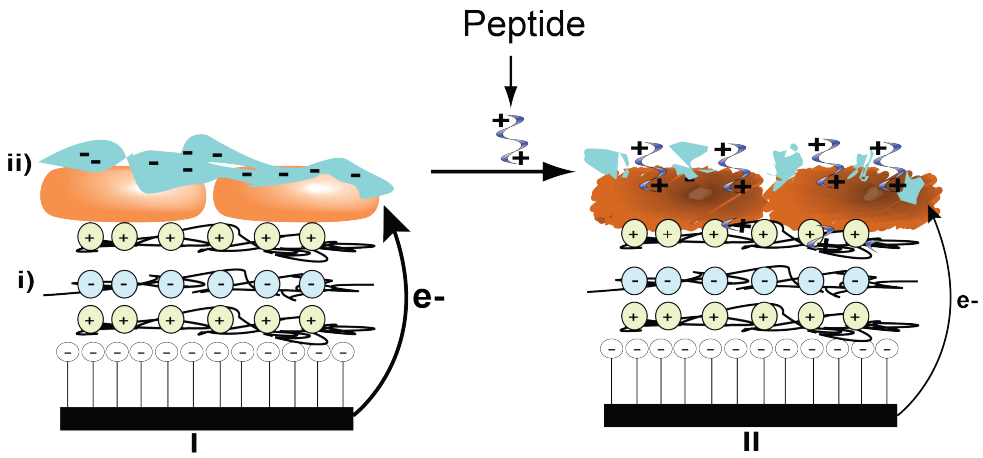

Scheme 5.1. Demonstration of processes resulting in current decrease at *Pseudomonas aeruginosa* modified electrode. I) a PG electrode modified with i) polymers and ii) *P. aeruginosa* provides large electrochemical responses due to the intact film containing pyocyanin. Upon exposure to peptide, II) the film is altered in such a way to cause the electrochemical signal to decrease significantly.

Whether the pyocyanin electrochemical peak decrease is due to bacterial death or a rearrangement of the film present on the electrode surface is not vitally important. What is important for the presentation here that this electrochemical signal is a convenient electrochemical handle to monitor the effectiveness of the AMP toward the destruction of the *P. aeruginosa* film. Coupling the data from Chapters 4 and 5, it is clear that these AMP are effective in destroying biofilm, and inhibiting its initial formation.

This process can be measured electrochemically based on the pyocyanin signal decrease, and the effectiveness of these AMP can be determined within a matter of minutes. Overall, the data presented here demonstrate that the electrochemical sensor is effective in determining the anti-biofilm activity of a series of AMP in a very rapid fashion for *P. aeruginosa* PAO1.

References

1. Webster TA, Sismaet HJ, Conte JL, Chan IP, Goluch ED. Electrochemical detection of pseudomonas aeruginosa in human fluid samples via pyocyanin. *Biosens. Bioelectron*. **2014**;*60*:265-270.

2. Hicks RP, Abercrombie JJ, Wong RK, Leung KP. *Bioorg. Med. Chem*. **2012**;*21*:205.

CHAPTER 6: FUTURE DIRECTIONS AND CONCLUSIONS

Future Directions

The natural future path of this research is to continue to test the effectiveness of the AMP toward other biofilm-forming bacteria. Figure 6.1 shows some preliminary

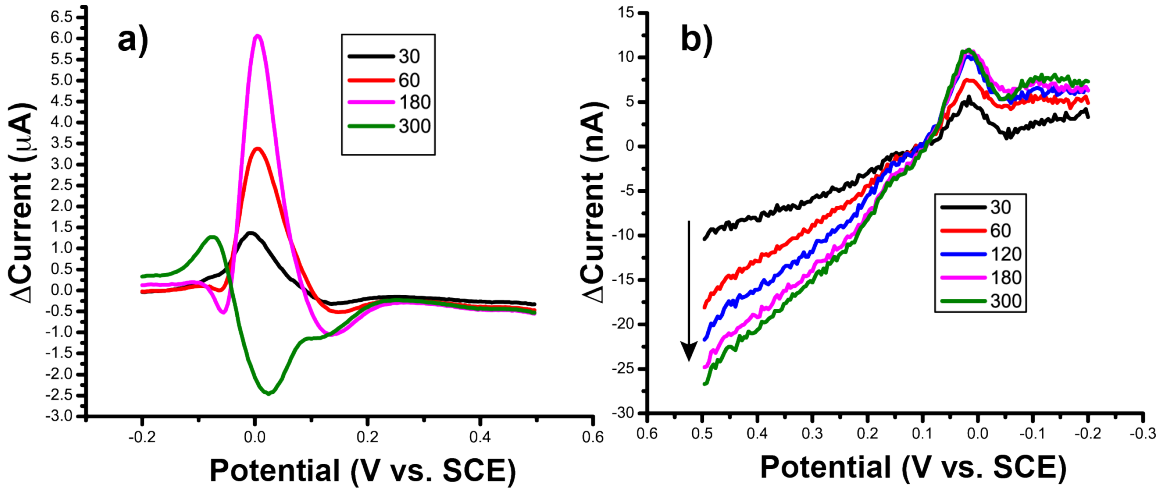

Figure 6.1. a) Background subtracted SWV showing voltammetric response of 400μM ferricyanide on a *Staphylococcus aureus*-modified electrode exposed to TTO-53 (1μM) for the denoted time in seconds. b) Similar plot without the added ferricyanide. Arrow denotes possible trend region – currents in the oxidative region decrease with additional TTO-53 exposure time. Conditions: Same as previously stated.

results employing *Staphylococcus aureus*-modified electrodes. These electrodes were formed in a similar manner as the *P. aeruginosa* electrodes then exposed to 1 mM TTO-53. Figure 6.1a shows the background subtracted response with added ferricyanide and Figure 6.1b shows the background subtracted response without the additional redox molecule. *S. aureus* is not electrochemically active like *P. aeruginosa*; therefore, the use of ferricyanide was thought to be necessary. An expected result might be the increase in

signal as the AMP compromises the biofilm in such a manner, allowing the ferricyanide to access the electrode. This is similar to our work presented in Chapter 3. However, as the figure shows, after the current increases up to 3 min TTO-53 exposure, an abrupt decrease in current is seen at 5 min. This behavior is not understood at this time.

The plot in Figure 6.1b shows similar data without the added ferricyanide. The response from *S. aureus* alone is much smaller; the current seen is nA vs. μA on the *P. aeruginosa* electrodes. While a small reduction peak does show up at ~0.00 V, and increases slightly over the course of the experiment, the current at positive potentials shows an interesting trend (arrow in the figure). This current decreases with TTO-53 exposure time, and it may provide a more useable metric to chart the viability of *P. aureus* vs. anti-biofilm agent exposure. Changes in this region might be due to the TTO-53 altering the film on the electrode surface, which changes the access of solution ions to the electrode, impacting the currents generated when acquiring the SWV. Additional experiments are necessary to ascertain if this is indeed due to the AMP exposure.

Overall, the data presented in Figure 6.1 demonstrate that this project is ripe with future possibilities. Each bacteria that is used to form the sensor will need to be optimized, the AMP will be tested for anti-biofilm properties toward the bacteria in question, and biological assays will need to be completed to show that the electrochemical assay results are meaningful. Additionally, other established anti-biofilm agents can be tested using the sensor platform. Once the parameters are established for important biofilm-forming bacteria, array formats and sensor miniaturization strategies can be explored.

Conclusions

Two electrochemical sensors have been developed for the purpose of testing the anti-biofilm activity of anti-microbial peptides containing unnatural amino acids. Both sensors were constructed utilizing LbL protocols. The first sensor utilized alginate as a *P. aeruginosa* biofilm mimic. Upon exposure to the peptides, an electrochemical signal increase over background was seen at approximately +0.07 V vs. Ag/AgCl as the peptides penetrated the alginate, exposing the underlying polymer layers to solution-phase ferricyanide. Based on these current changes, this sensor responded in the order TTO-23 > TTO-53 > TTO-45, which proceeds in order from longest carbon-chain linker (4) to ammonium group to the shortest (1). Control experiments showed that the combination of Tic-Oic amino acids and cationic charged side chains were both important for the peptide to penetrate the alginate layer.

Utilizing actual immobilized *P. aeruginosa* on the electrode surface, we showed that exposure to the peptides resulted in a current decrease over time. The bacteria was itself electroactive, and the current decrease was indicative of a change in the bacterial environment due to the peptide exposure. Additionally, TTO-53 was the most active toward altering the *P. aeruginosa* electrochemical response at lower concentrations, which is indicative of its anti-biofilm activity. This data was in better agreement with biological assays and previous results demonstrating that TTO-53 provided the most anti-*P. aeruginosa* biofilm activity and also the highest antimicrobial ability toward not only *P. aeruginosa*, but toward the ESKAPE pathogens in general. The findings and work presented here lay the foundation for a multitude of future studies related to anti-biofilm sensor development in the Hvastkovs lab at ECU.